Title
The Influence of Age and Alzheimer's Pathology on Hippocampal Function

Author
Marks, Shawn

Publication Date
2017

Peer reviewed|Thesis/dissertation

The Influence of Age and Alzheimer's Pathology on Hippocampal Function

By

Shawn M. Marks

A dissertation submitted in partial satisfaction of the

requirements for the degree of

Doctor of Philosophy

in

Neuroscience

in the

Graduate Division

of the

University of California, Berkeley

Committee in charge:

Professor William Jagust, Chair
Professor Mark D'Esposito
Professor Silvia Bunge
Professor Lexin Li

Summer 2017

Abstract

The Influence of Age and Alzheimer's Pathology on Hippocampal Function

By

Shawn M. Marks

Doctor of Philosophy in Neuroscience

University of California, Berkeley

Professor William Jagust, Chair

An abundance of research has demonstrated that aging is associated with declines in cognition, particularly episodic memory. A similarly large body of work has highlighted the underlying age-related functional alterations that occur within the hippocampus and surrounding medial temporal lobes (MTL) that may give rise to memory impairment. However, aging is also associated with the accumulation of Alzheimer's disease pathology, namely β-amyloid plaques (Aβ) and tau neurofibrillary tangles, which have been associated with a host of neural and behavioral changes, even in those without the disease. As such, it is unclear to what extent our understanding of age-related decline is attributable to the accumulation of pathology. Using a combination of neuropsychological assessment, structural and functional magnetic resonance imaging, and positron emission tomography, I will present two projects which seek to quantify hippocampal function in cognitively normal older adults, assess how Aβ and tau interact to alter neural activity, and define a functional mechanism through which pathology leads to episodic memory decline.

The first project focuses on a function commonly attributed to the hippocampus called pattern separation. Here, using a lure discrimination memory paradigm, I demonstrate that cognitively normal older adults exhibit a behavioral shift from pattern separation towards pattern completion that is associated with elevated neural activity in the hippocampus and MTL. Additionally, I show that Aβ and tau are uniquely associated with two measures of neural function during memory encoding, suggesting that Aβ and tau pathology likely interact to produce aberrant neural activity in older adults. In the second project, I use a technique called representational similarity analysis to explore the relationship between memory encoding and retrieval. Here, I demonstrate that older adults exhibit greater neural similarity between encoding and retrieval for incorrect lures (i.e. false alarm) relative to correct lures. I also demonstrate that false alarm similarity is associated with tau, but only in older adults without Aβ. This suggests that, independent of Aβ, tau can disrupt memory function, specifically by altering the relationship between neural activity during encoding and retrieval. In sum, this research indicates that Alzheimer's pathology alters hippocampal function in a way that leads to episodic memory impairment in cognitively normal older adults, and should be considered when addressing future questions about aging and memory.

Chapter 1: Introduction

1.1 Overview

I will begin in Chapter 1 by outlining the various memory systems thought to aid in recognition memory and the brain structures underlying these processes. Next, I will highlight a specific function of the hippocampus and offer evidence of its regional specificity. From there, I will discuss the neurobiological changes that occur in the aged hippocampus and explore how they manifest as functional and behavioral impairments. Finally, I will introduce Alzheimer's disease (AD) and describe the impact pathology has on the aging process. Chapters 2-4 will tie these themes together using data from my research.

1.2 Hippocampal Memory System

Human memory can be separated into two distinct components: declarative and nondeclarative memory. Declarative memory refers to the ability to recollect specific facts or events; whereas, nondeclarative memory refers to the ability to engage more implicit behaviors, such as habits, conditioning or priming (Schacter and Tulving, 1994; Squire and Zola, 1996). Declarative memory can be broken down further into semantic and episodic memory. Semantic memories contain factual knowledge free of other context (Tulving, 1972; Tulving et al., 1991). This is different from episodic memories, which describe events that can be associated with a specific time and place (Tulving, 2002). The process of forming new episodic memories is widely thought to rely on the hippocampus (Squire, 1992; Tulving and Markowitsch, 1998). Several frameworks have been proposed to describe episodic memory formation, but in general, most agree that the hippocampus acts by binding together the multidomain neural representations associated with an experience into a sparsely coded event (Moscovitch et al., 2016). To accurately recall an event, it is necessary to encode the experience in a way that reduces interference from other similar episodes (i.e. where you parked your car today versus yesterday). As such, computational models have proposed that the hippocampus performs a process called pattern separation (Marr, 1971; O'Reilly and McClelland, 1994; Treves and Rolls, 1994; Norman and O'Reilly, 2002; O'Reilly and Norman, 2002). Pattern separation refers to the orthogonalization of novel events into unique representations to reduce interference between previous experiences. This is contrasted by pattern completion, or the reactivation of neural representations when faced with partial or incomplete cues that aid in retrieval. In this framework, pattern separation may be more associated with recollection of events, while pattern completion may assist in event familiarity.

1.3 Other Medial Temporal Memory Systems

The hippocampus may act as a central hub for episodic memory, but it does not do so in isolation. Its neighboring regions in the medial temporal lobe (MTL), primarily the entorhinal, perirhinal and parahippocampal cortices, also play a significant role in memory processes. Recently, it has been suggested that the MTL memory system should be

broken into two unique subsystems (Ranganath and Ritchey, 2012). The anterior medial network relies heavily on the perirhinal cortex and has been implicated in familiarity-based recognition memory, emotional processing and social cognition, and semantic knowledge. The second, a posterior medial network, has the retrosplenial and parahippocampal cortices as core components and has been implicated in episodic memory retrieval, spatial navigation, and theory of mind. Under this framework, memory for the entities of an event (i.e. an object) would be dictated by the anterior temporal network, whereas memory for explicit details (i.e. space and time) might rely on the posterior temporal network. A similar dual-process model has suggested a division between the perirhinal and hippocampal memory systems (Brown and Aggleton, 2001; Aggleton and Brown, 2006). It posits that the perirhinal system is more rapid, automatic and tied to familiarity, while the hippocampal system is slower, associational and recollective in nature (see (Yonelinas, 2002) for a review of recollection and familiarity). Although we will focus extensively on the hippocampus and its role performing pattern separation, it is likely working in tandem with these other systems to produce successful memories.

1.4 Hippocampal Anatomy and Evidence of Pattern Separation

The emphasis on pattern separation in the hippocampus is a function of its unique anatomy and tri-synaptic circuitry. The hippocampus is located in the MTL as part of the brain's limbic system. It comprises the hippocampus proper, containing cornu Ammonis subfields CA1-CA4, dentate gyrus (DG) and subiculum (Duvernoy, 2005). The entorhinal cortex is the principal input into the hippocampus. Neurons from layer II of the entorhinal cortex project to the DG via the perforant pathway, with additional projections to the CA3 subfield. From there, granule cells in the DG project to the CA3 subfield via mossy fibers. Pyramidal cells in the CA3 subfield project heavily onto themselves via recurrent collaterals and onto the CA1 subfield via Schaffer collaterals. The output from the CA1 subfield is considered the main output of the hippocampus and travels through the subiculum and deep layers of the entorhinal cortex before reaching multimodal association cortices (Amaral and Lavenex, 2006). The sparse firing of DG granule cells suggests that they act as domain-agnostic pattern separators, quickly deciphering overlapping input from the entorhinal cortex (Barnes et al., 1990); whereas, the strong recurrent collaterals and weaker projections from the entorhinal cortex make the CA3 subfield an ideal candidate for pattern completion (Rolls, 1996). These interpretations have been largely supported by previous work in rats. Leutgeb et al. (2007) demonstrated that when rats were introduced to an environment that morphed from circle to square in seven, 10-minute increments, the firing fields of DG granule cells drastically changed with the environment. Meanwhile, the firing fields of simultaneously recorded CA3 neurons remained relatively stable until the environment was fully morphed from circle to square (Leutgeb et al., 2007). Recent work using fMRI has also provided evidence that pattern separation exists in DG/CA3 and can be elucidated using implicit and explicit lure discrimination tasks. Bakker et al. (2008) showed participants pictures of objects that were subsequently presented with an identical or lure pair. Activity in DG/CA3 for lure objects was significantly greater than repeated objects, but not significantly different than the first presentation in the lure pair. They interpreted the strong response to two unique

items in the lure pair to represent pattern separation. Taken together, both animal and human research lends credence to the idea that the hippocampus performs pattern separation to support episodic memory.

1.5 Aging and its Associated Changes

Although most cognitive domains deteriorate over time, episodic memory is highly susceptible to age-related decline. This may be in part due to the changes that occur locally within the hippocampus and MTL as we age. First, the DG and CA3 subfield receive fewer projections from the entorhinal cortex with age. Aged rats receive a third fewer synaptic contacts from the entorhinal cortex and the degree of memory impairment is associated with the extent of synaptic loss (Geinisman et al., 1992). Recent human work using diffusion tensor imaging (DTI) has demonstrated atrophy of the perforant pathway in older adults relative to young controls (Yassa et al., 2010a). Interestingly, the recurrent collaterals that project back onto the CA3 subfield are not reduced in aging (Smith et al., 2000). This suggests that there might be an age-related shift from pattern separation to completion due to changing neurobiology. Second, the hippocampus experiences less cholinergic modulation that is thought to aid in switching between encoding and retrieval. This reduction in modulation is associated with the degree of memory impairment (Chouinard et al., 1995; Nicolle et al., 1999). Third, all subregions of the aged hippocampus receive reduced inhibitory interneuron modulation (Vela et al., 2003; Stanley and Shetty, 2004). Coupled with reduced excitatory input from the entorhinal cortex, this likely disrupts the balance of excitation and inhibition that is crucial to hippocampal function. Lastly, synaptic plasticity is weakened in aged hippocampal neurons. Specifically, the perforant path connections to DG and CA3 are less excitable (Barnes et al., 1994) and require greater stimulation to induce long-term potentiation (Barnes et al., 2000). These small changes likely combine to create significant age-related memory decline.

To better understand how local changes in the hippocampus may manifest as behavior, elements of pattern separation have been explored in aged animals. Using a neurocognitive aging model in rats, it was observed that hippocampal neuron place fields robustly changed when young and memory-intact animals were exposed to environmental alterations. However, memory-impaired animals (those with the worst performance on the Morris water maze task) demonstrated place field ‘rigidity’ when exposed to changing environments. The extent of rigidity was associated with worse water maze performance (Wilson et al., 2003). These results offer evidence for how pattern separation changes with age, but it does not indicate regional specificity. Recent studies have since indicated that CA3 subfield neurons likely influence this rigidity. It was observed that aged CA3 place cells had higher firing rates in general, and failed to modulate firing rates and place fields when exposed to novel environments, when compared to young animals. This was contrasted by young and aged CA1 place cells that had similar firing characteristics in familiar and novel environments (Wilson et al., 2005). Higher firing rates in CA3 neurons are likely a function of decreased inhibitory input, which could reinforce the recurrent collaterals projecting back onto CA3 neurons and shift

behavior towards pattern completion. Unfortunately, since DG granule cells exhibit sparse firing patterns, results in aging have largely been limited to CA3 neurons.

The above age-related changes occur in the underlying neurobiology and are difficult to measure outside of animal models. As such, many researchers have taken to using fMRI to investigate episodic memory in older adult populations. One of the more common results is that aging is associated with increased hippocampal activation during a variety of memory paradigms. Specifically, Yassa et al. (2011) demonstrated that activity within the DG/CA3 was elevated in older adults for the contrast assessing correctly identified lure objects relative to incorrectly identified false alarms. The authors equated their findings with those observed in rats and suggested that this hyperactivity was reflective of a shift in behavior that favored pattern completion. However, there have also been studies that suggest that task-related activity decreases (Cabeza et al., 2004; Dennis et al., 2008) or remains unchanged (Sperling et al., 2003; Duverne et al., 2009; Persson et al., 2010) when compared to young controls. Cabeza and colleagues (2004) showed that hippocampal activity was reduced in older adults for tasks of working memory, visual memory and episodic retrieval. The disparity in results is likely a function of task and task difficulty, as well as varied participant and cohort demographics. Despite the results suggesting that increased hippocampal activation occurs in aging, the interpretation of the meaning of this finding has been debated. Some have argued that increased activation represents a compensatory mechanism which assists the aged brain in performing successful memory processes (Cabeza, 2002; Miller et al., 2008). Although plausible, this cannot be entirely true as studies have shown that increased activation is associated with worse performance on memory tasks (Yassa et al., 2011a), implying that this level of activity is inherently detrimental. Lastly, the studies mentioned thus far have focused primarily on task activation, but DTI has also been used to explore age-related memory impairment. Using a lure discrimination task as a behavioral index of pattern separation, it has been shown that both perforant pathway and fornix integrity is strongly associated with successful memory across the lifespan (Yassa et al., 2011b; Bennett et al., 2015; Bennett and Stark, 2016). When assessed together, the task activation and DTI results further confirm the work that has been done in animal models and provide a better understanding of how underlying neurobiological changes might lead to memory decline in adult humans.

Beyond normal age-related decline, individuals with mild cognitive impairment (MCI) also exhibit episodic memory impairment and elevated hippocampal activity during fMRI paradigms. Increased hippocampal activation has been observed when using a common face-name paradigm (Dickerson et al., 2005; Sperling, 2007), but also the same lure discrimination task that has been used to assess pattern separation mechanisms across the lifespan (Yassa et al., 2010b; Bakker et al., 2012). Bakker et al. (2012) noted that individuals with MCI showed increased activation in DG/CA3 relative to cognitively normal older adults and this activation was associated with worse memory overall. It was further confirmed that this level of activity was a detriment as the anti-epileptic drug levetiracetam could rescue performance while reducing neural activity in those with MCI. However, because MCI is thought to represent an intermediary between normal aging and AD, it is

uncertain to what extent these results are indicative of age-related processes or pathology.

1.6 Alzheimer's Disease and its Relation to Aging

The most prominent clinical symptom of AD is episodic memory impairment, but at a molecular level, AD is characterized by the accumulation of two aggregated proteins: β-amyloid (Aβ) and tau. Aβ peptides are naturally occurring byproducts of metabolism, but it is believed that an imbalance between production and clearance leads to the accumulation of peptides, causing the formation of Aβ plaques. The accumulation of diffuse Aβ into plaques has been suggested as the initiating factor of AD (Hardy and Higgins, 1992; Hardy, 2009). Plaques occur when Aβ arranges itself into insoluble β-pleated sheets, surrounded by degenerating and dystrophic neurites, but Aβ can also exist as smaller oligomers (2-6 peptides). These soluble forms of Aβ have been shown to be toxic to synapses (Walsh et al., 2002; Cleary et al., 2004; Shankar et al., 2007) and are secreted with neural stimulation (Cirrito et al., 2005; Bero et al., 2011). In fact, Aβ is believed to be excitotoxic (Mattson et al., 1992; Harkany et al., 2000), potentially leading to a deadly cycle alternating between activation and further Aβ secretion. Busche et al. (2008) nicely demonstrated that transgenic mice expressing Aβ plaques had a higher proportion of hyperactive cortical neurons than their wildtype counterparts. A follow-up study further demonstrated that Aβ plaques led to hippocampal hyperactivity (Busche et al., 2012), offering a possible explanation for age-related memory impairment.

Tau is a microtubule-associated protein that, when hyperphosphorylated, aggregates into paired helical filaments that form neurofibrillary tangles within pyramidal neurons. The number of tangles is a common marker of AD severity, and much like Aβ, abnormal aggregates of tau have been shown to be toxic (Khlistunova et al., 2006), and associated with impaired cognition (Arriagada et al., 1992; Giannakopoulos et al., 2003) and neuronal loss (Gomez-Isla et al., 1997). Work in transgenic mice suggests that the formation of tau neurofibrillary tangles occurs after the accumulation of Aβ (Götz et al., 2001; Oddo et al., 2003), but that Aβ-induced toxicity is dependent upon tau (Rapoport et al., 2002; Roberson et al., 2007; 2011). This suggests that Aβ and tau interact to cause functional and behavioral changes in the aging brain. Recent work has suggested, however, that the accumulation of tau, in the absence of Aβ, can also produce memory impairment (Crary et al., 2014). Because tau first accumulates in the MTL (Braak and Braak, 1991), there is reason to suspect a tau-specific mechanism exists that can produce episodic memory dysfunction.

Importantly, both Aβ and tau pathology begin to accumulate during midlife, years prior to the onset of disease symptomology (Braak and Braak, 1997; Bennett et al., 2006). As such, some degree of age-related memory decline may be a result of the accumulation of AD pathology in cognitively normal older adults. Over the past decade, researchers have relied on PET imaging to quantify AD pathology in older adults, but work has primarily been limited to the investigation of Aβ. A growing number of studies have shown that increased Aβ, as measured with PET, is associated with altered neural function

during episodic memory paradigms. Specifically, Aβ has been linked to increased hippocampal activity (Mormino et al., 2012; Huijbers et al., 2015), increased entorhinal activity (Huijbers et al., 2014), reduced task-induced deactivations (Vannini et al., 2012a), inability to modulate encoding/retrieval activity (Vannini et al., 2012b), and impaired default mode network function (Sperling et al., 2009). However, these studies do not account for the presence of tau pathology in their older adult cohorts, preventing a complete understanding of how the two pathologies interact to cause impairment. Only recently has a radiotracer been developed that is capable of measuring tau pathology. As a result, little has been done outside of characterizing the spread of tau *in vivo* (Cho et al., 2016; Schöll et al., 2016; Schwarz et al., 2016) and assessing its relationship with cognition (Ossenkoppele et al., 2016; Saint-Aubert et al., 2016).

1.7 Overarching Questions

As there have been conflicting results describing neural function during episodic memory paradigms in cognitively normal older adults, I first sought to explore the robustness of the finding that aging is associated with increased hippocampal activity, particularly in the context of pattern separation. Second, I asked whether the accumulation of Aβ and tau pathology could account for changes in the underlying brain function during episodic memory encoding. Until recently, it has not been possible to quantify both pathologies *in vivo* and it was important to explore how they might interact in the context of a memory task. Both questions are addressed in Chapter 2, as well as a detailed look at how neural function and pathology relate to cognition and brain structure.

Finally, although an extensive body of work exists to suggest that AD pathology is associated with cognitive decline, little work has been done to describe, mechanistically, how this may manifest in cognitively normal older adults. Building from results presented in Chapter 2, I sought to explore how Aβ and tau pathology alter the relationship between episodic memory encoding and retrieval. In Chapter 3, I aimed to address this question by leveraging a technique called representational similarity and offer evidence for a tau-specific mechanism for memory impairment.

Chapter 2: Tau and β-amyloid are associated with medial temporal lobe structure, function and memory encoding in normal aging

2.1 Overview

Normal aging is associated with decline in episodic memory, and also with aggregation of the β-amyloid (Aβ) and tau proteins and atrophy of medial temporal lobe structures crucial to memory formation. While some evidence suggests that Aβ is associated with aberrant neural activity, the relationships between these two aggregated proteins, neural function, and brain structure are poorly understood. Using in vivo human Aβ and tau imaging, we demonstrate that increased Aβ and tau are both associated with aberrant functional magnetic resonance imaging activity in the medial temporal lobes during memory encoding in cognitively normal older adults. This pathological neural activity was, in turn, associated with worse memory performance and atrophy within the medial temporal lobes. A mediation analysis revealed that the relationship with regional atrophy was explained by medial temporal lobe tau. These findings broaden the concept of cognitive aging to include evidence of Alzheimer's disease-related protein aggregation as an underlying mechanism of age-related memory impairment.

2.2 Significance

Alterations in episodic memory, and the accumulation of Alzheimer's pathology, are common in cognitively normal older adults. However, evidence of pathological effects on episodic memory has largely been limited to Aβ. Since Aβ and tau often co-occur in older adults, previous research offers an incomplete understanding of the relationship between pathology and episodic memory. With the recent development of *in vivo* tau PET radiotracers, we show that Aβ and tau are associated with different aspects of memory encoding, leading to aberrant neural activity that is behaviorally detrimental. Additionally, our results provide evidence linking Aβ and tau associated neural dysfunction to brain atrophy.

2.3 Introduction

Successful episodic memory processes require a large-scale network of medial temporal lobe (MTL) structures, central to which are the hippocampus and entorhinal cortex. This network is highly susceptible to age-related decline, as evidenced by changes in cognition, structure, and function. Older adults often have difficulty forming new memories (Small et al., 1999; Hedden and Gabrieli, 2004), and neuroimaging studies have repeatedly found that MTL volumes decrease across the lifespan (Jernigan et al., 1991; Pruessner et al., 2001; Raz et al., 2004). The structures leveraged by the episodic memory network are also disrupted in Alzheimer's disease (AD). The formation of tau neurofibrillary tangles is first seen in the transentorhinal and entorhinal cortex (Braak and Braak, 1991; 1997); while, Aβ plaques accumulate in a number of neocortical regions that

are ultimately reciprocally connected to the hippocampus via the entorhinal cortex and perforant pathway (Braak and Braak, 1991; Thal et al., 2002). In conjunction with these two aggregated proteins, atrophy of the hippocampus and entorhinal cortex are hallmarks of the disease (Laakso et al., 1996; Scheltens, 2001).

Recent fMRI studies of age-related memory decline have demonstrated that hippocampal hyperactivity is often observed in older adults when compared to young controls (Miller et al., 2008; Yassa et al., 2011a). As AD pathology is commonly observed in cognitively normal individuals (Bennett et al., 2006), some degree of what is considered as normal age-related decline may be attributable to AD pathology. In fact, multiple studies have reported alterations in the hippocampal memory network that are associated with Aβ. Elevated Aβ has been linked to increased hippocampal activation (Mormino et al., 2012), increased entorhinal cortex activation (Huijbers et al., 2014), and reduced task-induced deactivation (Sperling et al., 2009) in cognitively normal older adults. Aβ is thought to be excitotoxic, potentially leading to aberrant cellular activity (Mattson et al., 1992; Busche et al., 2008); however, Aβ is unlikely to be the sole contributor to memory impairment. Tau is more closely associated with AD symptoms than is Aβ (Arriagada et al., 1992; van Rossum et al., 2012), and while MTL tau pathology is common as an isolated pathology in older people (Crary et al., 2014), Aβ often co-occurs with tau pathology (Price and Morris, 1999; Chabrier et al., 2012) and may be involved in its spread to neocortex (Schöll et al., 2016). Neuroimaging studies to date have been limited in that they do not fully account for the role of both Aβ and tau in relation to MTL function.

To examine the effect of AD pathology on memory network function and decline in normal aging, we used a lure discrimination paradigm specifically designed to tax the hippocampal formation. A core function of the hippocampus is to orthogonalize information into noncompeting representations, or pattern separation (Marr, 1971; Treves and Rolls, 1994; O'Reilly and Norman, 2002). Yet older adults, when confronted with stimuli that are similar but not identical to those previously observed, frequently misidentify these lures as older representations (pattern completion). This age-related behavioral change has been associated with both increased hippocampal activation and structural degradation of the perforant pathway and limbic tracts, potentially disconnecting hippocampus from neocortex (Yassa et al., 2010a; 2011a; Bennett et al., 2015). Since tau accumulation in cognitively normal older adults usually occurs in the entorhinal cortex and hippocampus (Braak and Braak, 1997), a reasonable hypothesis is that tau accumulation provokes hippocampal dysfunction and produces memory impairment in aging. In addition, our previous work, as well as work in other laboratories cited above, implicates Aβ involvement in hippocampal hyperactivation. Our goal therefore was to explore relationships between tau and Aβ accumulation, measured with ^{18}F-AV-1451 (Xia et al., 2013) and ^{11}C-Pittsburgh Compound B (PIB) PET (Price et al., 2005), to task-related brain activation, episodic memory, and brain structure in cognitively normal older adults. We hypothesized that increased task-related activation would be associated with impaired cognitive performance, atrophy of the MTL, and both tau and Aβ.

2.4 Materials and Methods

2.4.1 Participants

Sixty healthy older adults aged 64-93 years (OA; 40 female) and 24 young adults aged 18-30 years (YA; 16 female) were recruited from the Berkeley Aging Cohort, an ongoing longitudinal study of cognitive aging, to participate in PET and MRI imaging. All participants underwent a detailed medical interview and battery of neuropsychological assessments prior to enrollment. To be eligible, OA were required to be 64 years of age or older, living independently in the community, free of neurological and major medical illness, and have normal performance on neuropsychological tests (within 1.5 SD of the mean). Seventeen OA and 4 YA were excluded because of poor performance (below chance on lure discrimination, n = 2), problems with data collection (behavioral and MRI, n = 8) or image normalization (n = 3), and excessive motion (n = 8), resulting in 43 OA and 20 YA for subsequent data analysis (Table 1). All OA received MRI and ^{11}C-PIB PET for amyloid imaging, while a subset received ^{18}F-AV-1451 PET (n = 35) for tau imaging. YA only participated in MRI imaging. MRI scans were acquired within an average of 97.58±94.81 days from PIB and 123.66±198.97 days from AV-1451 PET scans. All participants provided informed consent in accordance with the Institutional Review Boards of the University of California, Berkeley, and the Lawrence Berkeley National Laboratory (LBNL).

Table 1. Participant Demographics

	Young Adults	Older Adults
n	20	43
Age	23.25 (3.21)	78.80 (5.75)
Sex (M/F)	7 / 13	12 / 31
Education	15.21 (1.58)[a]	16.63 (1.98)
MMSE	29.00 (1.26)	28.86 (1.21)
APOE (0/1/2 ε4 allele)	N/A	28 / 14 / 0 (1 N/A)
PIB DVR	N/A	1.12 (0.18)
AV-1451 SUVR (Braak I/II)	N/A	1.51 (0.19)
Days between MRI and PIB	N/A	97.58 (94.81)
Days between MRI and AV-1451	N/A	123.66 (198.97)

All values are mean (SD) unless stated otherwise. MMSE, Mini-Mental State Examination; *APOE*, Apolipoprotein E; DVR, distribution volume ratio; SUVR, standard uptake value ratio.
[a]Significantly different from older adults (two-sample *t*-test, p < 0.05)

2.4.2 Behavioral Task

The episodic memory paradigm used was adapted from Yassa et al. (2011). Across six runs in the scanner, participants were shown color photographs of novel, repeated, and

similar (i.e. lure) objects. Participants were told to identify the objects seen as new (first), old (repeat), or similar but not identical (lure). Objects were presented one at a time for 2000 ms, followed by a black fixation cross with a fixed 500 ms inter-trial interval. Each run contained 16 repeated pairs, 16 lure pairs and 44 novel objects, with no objects duplicated between runs. Objects were fully randomized and the distance between repeated and lure pairs was randomly varied between 10 and 40 trials. PsychoPy (www.psychopy.org) was used for stimulus presentation and behavioral data collection.

2.4.3 PET Acquisition

PIB was synthesized at the LBNL Biomedical Isotope Facility. PIB-PET imaging was performed at LBNL using an ECAT EXACT HR or BIOGRAPH PET/CT Truepoint 6 scanner (Siemens Medical Systems) in three-dimensional acquisition mode. Thirty-five dynamic acquisition frames were obtained over 90 minutes (4 × 15 s, 8 × 30 s, 9 × 60 s, 2 × 180 s, 10 × 300 s and 2 × 600 s) immediately following injection of 10-15mCi of PIB into an antecubital vein. Ten-minute transmission scans for attenuation correction or X-ray CT were obtained for each PIB scan. Data were reconstructed using an ordered subset expectation maximization algorithm with weighted attenuation and smoothed with a 4 mm Gaussian kernel with scatter correction.

AV-1451 was synthesized at LBNL using a GE TracerLab FXN-Pro synthesis module with a modified protocol based on that supplied by Avid Radiopharmaceuticals. AV-1451 PET imaging was performed on the BIOGRAPH PET/CT scanner. Following the injection of 10 mCi of AV-1451, one of two acquisition schemes were acquired: 0-100 minutes of dynamic data (4 x 15 s, 8 x 30s, 9 x 60 s, 2 x 180 s and 16 x 300 s frames), followed by 120-150 minutes (6 x 300 s frames, n = 18), or 75-115 minutes (8 x 300 s frames, n = 17). Analyzed data from both acquisition schemes used only frames from 80-100 min. A CT scan was performed before the start of each emission acquisition. Data were reconstructed using an ordered subset expectation maximization algorithm with weighted attenuation and smoothed with a 4 mm Gaussian kernel with scatter correction.

2.4.4 MRI Acquisition

High-resolution fMRI was performed at the Henry H. Wheeler Jr. Brain Imaging Center (BIC) on a 3T TIM/Trio scanner (Siemens Medical Systems) using a 32-channel head coil. Each of the six functional runs utilized a T2*-weighted echo-planar imaging sequence (TR = 1500 ms; TE = 34 ms; flip angle = 70°; matrix = 132 x 132; FOV = 200; voxel size = 1.5 x 1.5 x 1.5 mm; duration = 5 min). A parallel imaging reduction factor of 2 was used to reduce acquisition time and minimize distortion due to magnetic susceptibilities near the temporal lobes. Nineteen slices oriented parallel to the primary axis of the hippocampus were acquired in interleaved order, covering the entirety of the MTL. One hundred ninety-six volumes were acquired during each run. The first ten volumes were discarded as they were used to ensure signal equilibrium and minimal subject motion during the parallel imaging normalization template acquisition. A T1-weighted volumetric magnetization prepared rapid gradient echo image (MPRAGE; TR = 2300 ms; TE = 2.98 ms; matrix = 256 x 256; FOV = 256; sagittal plane; voxel size = 1 x 1 x 1 mm; 160 slices)

was collected and used during coregistration of functional data. An MPRAGE image (TR = 2,110 ms; TE = 3.58 ms; matrix = 256 × 256; FOV = 256; sagittal plane; voxel size = 1 × 1 × 1 mm; 160 slices) was also collected at LBNL on a 1.5T Magnetom Avanto (Siemens Medical Systems) for PET coregistration purposes.

2.4.5 PET Processing

PET data were processed using the SPM12 software package (RRID:SCR_007037). PIB-PET data were realigned and frames corresponding to the first 20 minutes of acquisition were averaged and used to guide coregistration with the participant's LBNL MPRAGE. The coregistration matrix was applied to realigned frames and data were resliced to MRI space. Distribution volume ratio (DVR) images of PIB-PET data 35-90 minutes post-injection were created using Logan graphical analysis and a FreeSurfer derived grey cerebellum reference region (Logan, 2000). Global PIB DVR values were calculated for each participant, defined as the mean DVR within regions of interest (ROI) in frontal, parietal, temporal and cingulate cortices (Mormino et al., 2011). Previous work demonstrated that global PIB DVR values did not significantly differ between the two scanners used for data collection (Elman et al., 2014).

AV-1451-PET data were realigned and the mean of all frames was used to coregister data to the participant's LBNL MPRAGE. Standard uptake value (SUV) images representing data 80-100 minutes post-injection were created and normalized by a grey cerebellum reference region to generate native space SUV ratio (SUVR) images. SUVR images were partial volume corrected using the Rousset approach (Rousset et al., 1998). Volume-weighted mean SUVR values within anatomically approximated Braak staging were calculated using a previously described method (Schöll et al., 2016). Briefly, Braak ROIs were created by combining FreeSurfer segmentations (see below) into non-overlapping stages used to describe AD-related tau pathology (i.e. I/II transentorhinal, III/IV limbic and V/VI isocortical).

2.4.6 MRI Processing

BIC and LBNL MPRAGE data were processed using FreeSurfer version 5.3 (RRID:SCR_001847) to define native space ROIs for each participant (Dale et al., 1999; Fischl et al., 2001; 2002; Ségonne et al., 2004). FreeSurfer ROIs obtained using LBNL data were used to create Braak ROIs and calculate PIB DVR values. FreeSurfer ROIs obtained using BIC data were used to measure thickness of MTL subregions, averaged across hemispheres. Hippocampus and entorhinal, parahippocampal and perirhinal cortices were manually segmented for each participant on BIC MPRAGE images following previously established guidelines (Insausti et al., 1998; Pruessner et al., 2002; Duvernoy, 2005). These segmentations were used to quantify average hippocampal volume. Hippocampal volume was corrected for total intracranial volume (ICV) using a covariance approach, as defined by the following formula: adjusted volume = raw volume – beta * (ICV – mean ICV), with beta being the regression coefficient when raw volume is regressed against ICV, and mean ICV represents the group average (Mathalon et al., 1993).

2.4.7 fMRI Processing

fMRI data were processed and analyzed using a combination of Advanced Normalization Tools (RRID:SCR_004757) and SPM12. For a given run, images were realigned to the first volume and smoothed with a 5 mm Gaussian kernel. Motion vectors were created and used to identify significant motion spikes (greater than 2 mm displacement, plus and minus one TR). A mean fMRI image was created, bias corrected, and thresholded to exclude surrounding non-brain tissue and skull. The resulting image was used in a two-step spatial normalization process. First, the mean fMRI image was linearly registered to the participant's skull-stripped, BIC MPRAGE. Second, the BIC MPRAGE was nonlinearly registered to the skull-stripped MNI ICBM 152 Nonlinear Asymmetric template (Fonov et al., 2009). The two transformations were combined and applied to the participant's fMRI data as one transformation.

2.4.8 fMRI Analysis

Individual runs were modeled using FSL's FEAT version 6.0 (RRID:SCR_002823). Trials were categorized into eight bins. Four of these represented activity upon the first presentation of the stimuli: (1) novel objects (stimuli presented only once), (2) subsequent hits, (3) subsequent correct rejections, and (4) subsequent false alarms. Three represented activity upon presentation of the paired stimuli: (5) hits (repeat presentation correctly identified as old), (6) correct rejections (lure presentations correctly identified as similar), (7) false alarms (lure presentations incorrectly identified as old), with an 8^{th} category of errors and omissions. Data were convolved with a double gamma hemodynamic response function, and each bin, their corresponding temporal derivatives, six rigid body motion parameters, and outlier volumes (those with excessive motion) were entered in a general linear model to predict fMRI signal. The resulting contrasts reflect activity for a given task-related bin relative to the non-zero, novel object baseline condition. Second-level contrasts were created for each participant by combining all six runs using a one-sample *t*-test with fixed effects. Third-level group statistics were created for all subsequent hits, subsequent correct rejections, and subsequent false alarms by combining all individual subject data using one-sample *t*-tests. All third-level statistics were masked to only include hippocampus, and entorhinal, parahippocampal and perirhinal cortices (98,256 1.5mm^3 voxels), as defined above, and a threshold of $p < 0.05$ uncorrected and $k \geq 250$ cluster extent was employed. Each condition's significant activations or deactivations were binarized and used to extract data from individual participants. Differences between groups were quantified using two-sample *t*-tests.

2.4.9 Statistical Analyses

Statistical analyses and plots were performed using R version 3.2.3 (RRID:SCR_001905). Group differences were assessed using *t*-tests. Multiple regression was used to assess relationships between cognition, task activation, and biomarker data within OA. All regression analyses were controlled for age, sex and education. Regression models involving PET biomarkers were additionally controlled for hippocampal volume to account for spatial resolution differences between high-resolution

fMRI and PET. Mediation analyses were performed using the 'mediation' package in R. Dice's coefficient was calculated to quantify the similarity between clusters of task-related activation. Significant relationships were reported at $p < 0.05$ and trends of $p < 0.1$ were addressed.

2.5 Results

2.5.1 Memory Performance

All participants were administered the memory paradigm outlined in Figure 2.1A during fMRI data acquisition. Differences were found between OA and YA for all but one behavioral condition, repeated objects called new, with the most pronounced differences seen for lure objects called similar (Figure 2.1B). To assess task performance, a lure discrimination index (LDI) was defined as [p(similar|lure) + p(new|lure)] – p(similar|first). This measure generally describes the likelihood that a lure was correctly identified and corrects for response bias within participants. Overall, OA performed worse when compared to YA (t_{52} = -5.70, $p < 0.001$; Figure 2.1C).

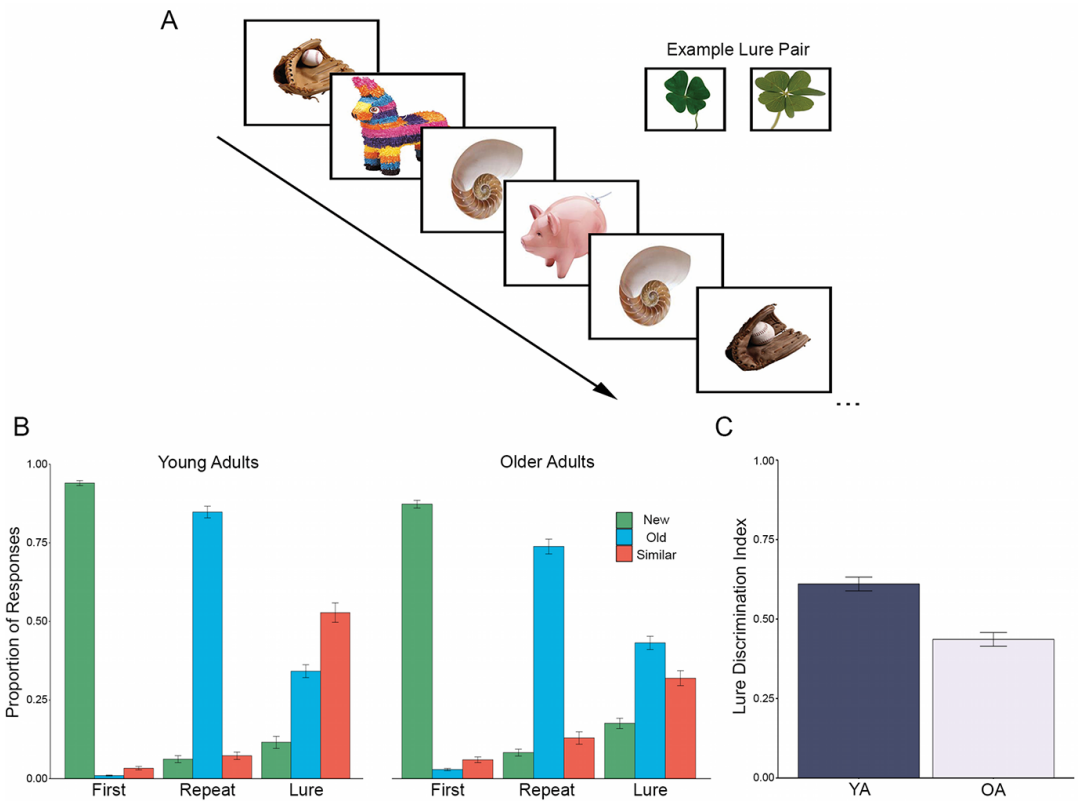

Figure 2.1. Lure discrimination paradigm and behavioral performance. (A) Participants were instructed to identify objects as being new (first presentation of object), old (repeated object), or similar (lure object resembling a previous trial). Objects were presented for 2000 ms followed by a 500 ms inter-trial interval. Similar lures acted as the primary trials for assessing memory performance. (B) Proportion of response for each trial type. Responses to all trial types differed between young and older adults, with older adults generally performing worse. (C) The lure discrimination index, quantifying the likelihood of correctly identifying lure objects, was significantly lower for older adults (OA) compared to young adults (YA). Data presented as means ± standard error.

2.5.2 Activation and Deactivation Patterns in Older Adults

Neural activity during stimulus encoding for 3 conditions was compared to activity for novel stimuli presented only once using one-sample *t*-tests in the OA group (Figure 2.2). Activations associated with subsequent hits (sH; correctly identified as old on the subsequent presentation) were found in left entorhinal cortex and bilateral parahippocampal cortex. Clusters of sH deactivations were found in left perirhinal cortex near the border of the entorhinal cortex, bilateral anterior hippocampus, and right posterior hippocampus. For subsequent correct rejections (sCR; correctly identified as similar on the subsequent presentation), activations were found in bilateral perirhinal cortex, left anterior hippocampus, left posterior hippocampus, and right parahippocampal cortex. No clusters of voxels exceeded the threshold for deactivations. Subsequent false alarm (sFA; subsequently incorrectly identified as old upon presentation of a lure) activations were found in bilateral perirhinal cortex, left anterior hippocampus, left posterior hippocampus, left parahippocampal cortex, and right entorhinal cortex. sFA deactivations were found in right entorhinal cortex, and right anterior and posterior hippocampus.

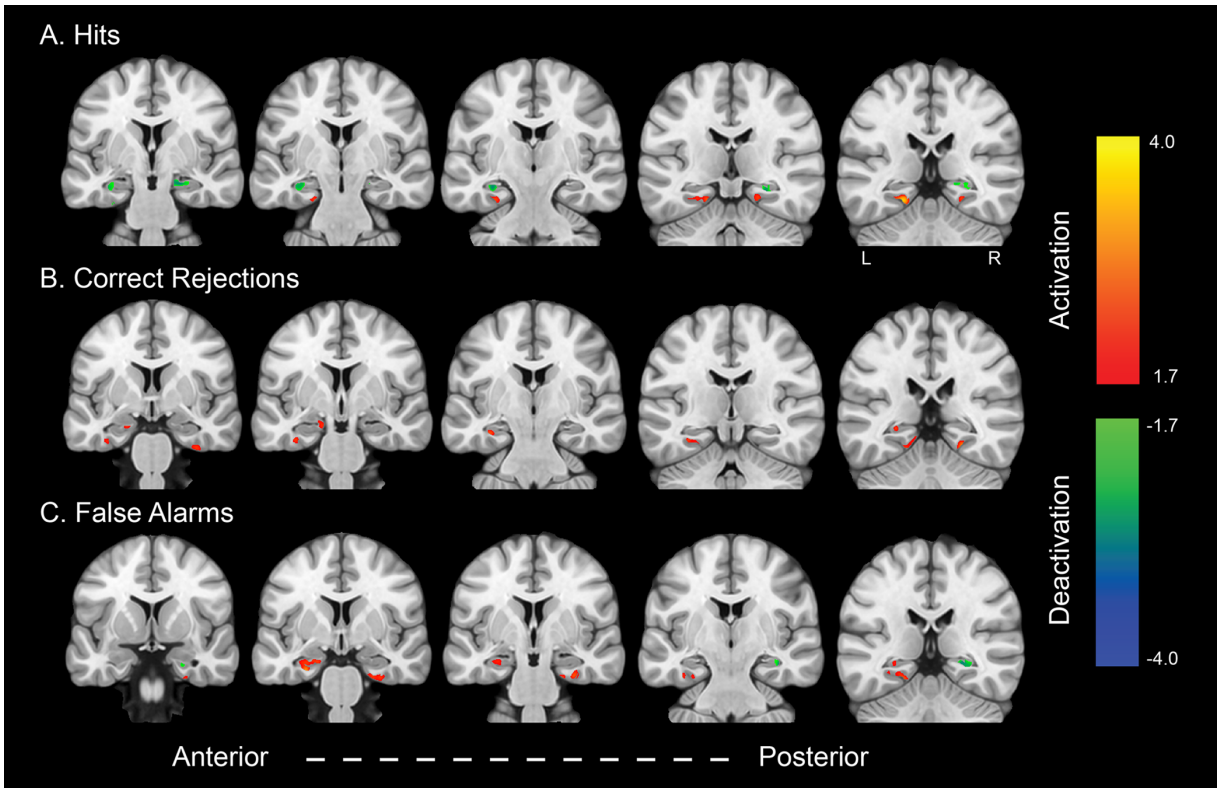

Figure 2.2. Patterns of fMRI activation during memory encoding in older adults. One-sample *t*-tests of activation (shown in warm colors) and deactivation (shown in cool colors) in older adults during trials of subsequent hits (A; sH), subsequent correct rejections (B; sCR), and subsequent false alarms (C; sFA) compared to novel stimuli presented only once. Data represented as *t*-statistics and masked to included only hippocampus and perirhinal, entorhinal, and parahippocampal cortices.

2.5.3 Differences in Activation and Deactivation Patterns between Older and Young Adults

To determine if neural activity differed between OA and YA groups, we first quantified activity in YA within the contrasts identified using one-sample *t*-tests of OA participants. When compared to OA, YA had significantly reduced activation in the sH (t_{43} = -2.58, p = 0.01) and sFA (t_{54} = -3.64, p < 0.001) contrasts. A non-significant trend was observed in the sCR contrast (t_{30} = -1.88, p = 0.07). Additionally, we performed two-sample *t*-tests to explore explicit differences between groups (Figure 2.3). Numerous clusters of increased activation were found in OA for all trial types. Specifically, clusters were found in right anterior hippocampus, bilateral entorhinal and bilateral parahippocampal cortex for sH, bilateral hippocampus (both anterior and posterior) and right parahippocampal cortex for sCR, and right entorhinal cortex, bilateral anterior hippocampus and bilateral parahippocampal cortex for sFA. Only one cluster of activity in left anterior hippocampus was associated with increased activity in YA during sH trials. Finally, we sought to compare patterns of activation derived from both analyses by calculating Dice's coefficient for each trial type. Values associated with sH, sCR, and sFA activations were calculated to be 0.28, 0.10, and 0.45, respectively. Although these values indicate the two analyses do not completely overlap, there is likely shared neural activity between groups that may not arise using *t*-tests, but is required to perform lure discrimination. As such, we chose to assess further relationships with task-related activation using the contrasts defined within OA participants only.

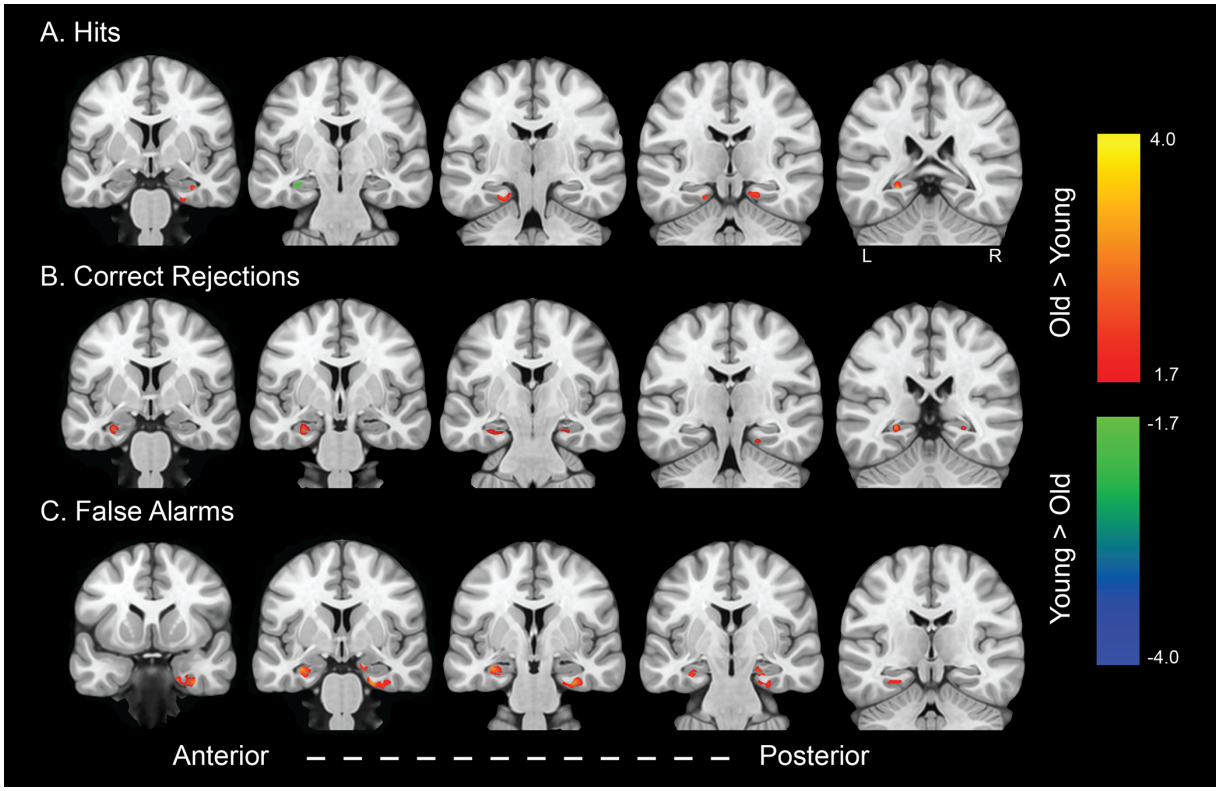

Figure 2.3. Differences in fMRI activation during memory encoding between older and young adults. Patterns of activation associated with group difference between older adults (shown in warm colors) and young adults (shown in cool colors) during trials of

subsequent hits (A; sH), subsequent correct rejections (B; sCR), and subsequent false alarms (C; sFA). Data represented as *t*-statistics and masked to included only hippocampus and perirhinal, entorhinal, and parahippocampal cortices.

2.5.4 Amyloid and Tau Characteristics in Older Adults

Approximately 45% of OA were classified as Aβ+ using a cutoff of 1.07, which has been detailed previously (Villeneuve et al., 2015). This percentage is higher than most studies of cognitively normal older adults as the participants were recruited in order to enrich for Aβ, to better test our hypotheses. Tau was quantified into three measures that closely approximated anatomically defined Braak staging. Specifically, Braak I/II contained entorhinal cortex and hippocampus, Braak III/IV contained limbic structures including inferior temporal cortex, amygdala and thalamus, and Braak V/VI contained isocortical structures including frontal, parietal and occipital cortices. Of the 35 total participants included in analyses, 6 OA were classified as Braak 0, 23 OA were classified as Braak I/II, and 6 OA were classified as Braak III/IV. No OA had substantial tau in Braak V/VI regions. As the majority of OA had tau deposition in the Braak I/II regions, the other stages were excluded from further analyses. Age was significantly associated with Braak I/II tau such that older participants had more tau (r_{33} = 0.48, p = 0.002). Representative PIB and AV-1451 images are shown in Figure 2.4.

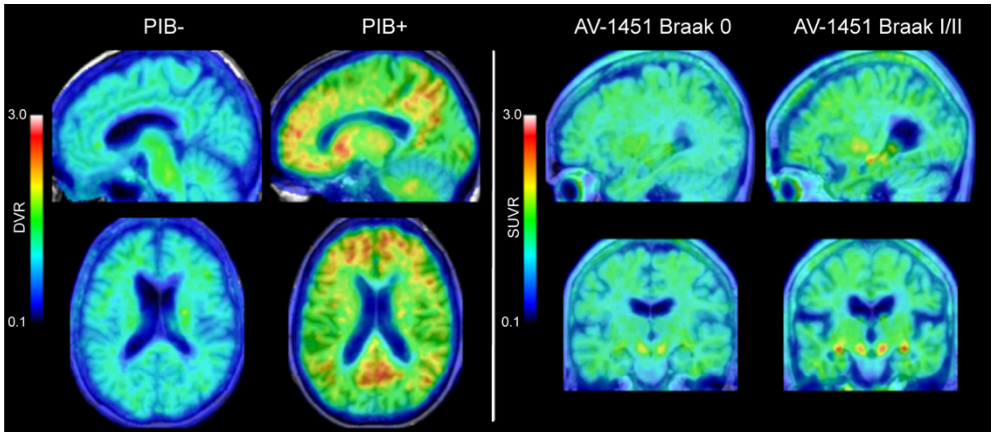

Figure 2.4. PIB and AV-1451 PET imaging. Distribution volume ratio (DVR) and standard uptake value ratio (SUVR) images of PIB and AV-1451 binding in representative participants. Areas of significant Aβ burden were seen in frontal and parietal cortices, and posterior cingulate. Significant tau burden was largely restricted to the medial temporal lobes.

2.5.5 Relationships with Task Specific Activation

In order to determine whether early AD pathology influences brain function during memory encoding, we sought to relate measures of tau and Aβ pathology with task-related activation. No significant relationships were found with sCR activations. Reduced sH deactivation was associated with increased global PIB DVRs (r_{36} = 0.47, p = 0.05; Figure 2.5A), with females deactivating more than males (t_{28} = -2.77, p = 0.01). Increased activations during sFA were associated with elevated tau in Braak I/II (r_{28} = 0.41, p = 0.01; Figure 2.5B). The results would not survive a Bonferroni adjusted p-value of 0.005.

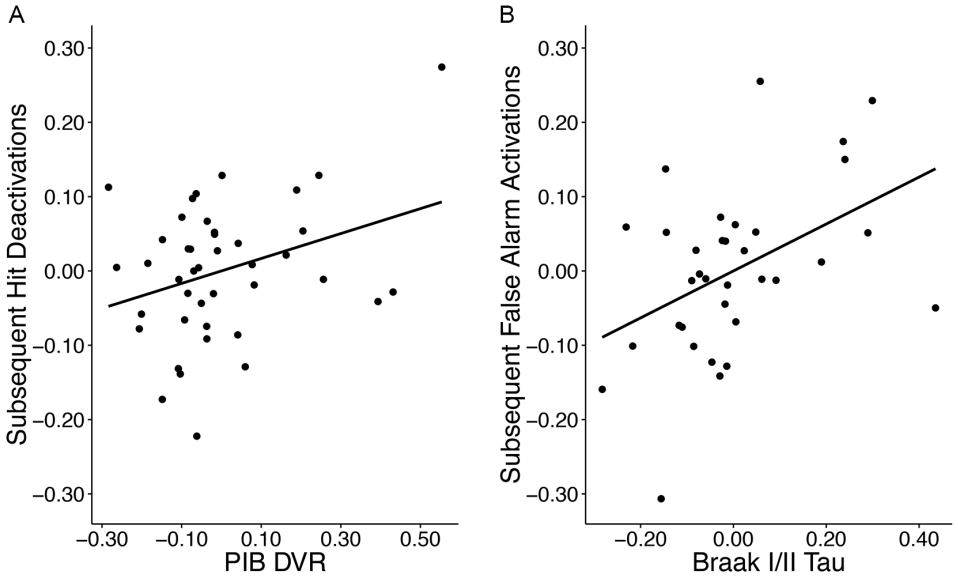

Figure 2.5. Relationship between fMRI activation and Alzheimer's pathology. (A) Positive relationship between PIB distribution volume ratio (measure of β-amyloid) and subsequent hit deactivation (r_{36} = 0.47, p = 0.05). (B) Positive relationship between AV-1451 Braak I/II standard uptake volume ratio (measure of tau) and subsequent false alarm activation (r_{28} = 0.41, p = 0.01). Data are residuals controlling for age, sex, education, and hippocampal volume.

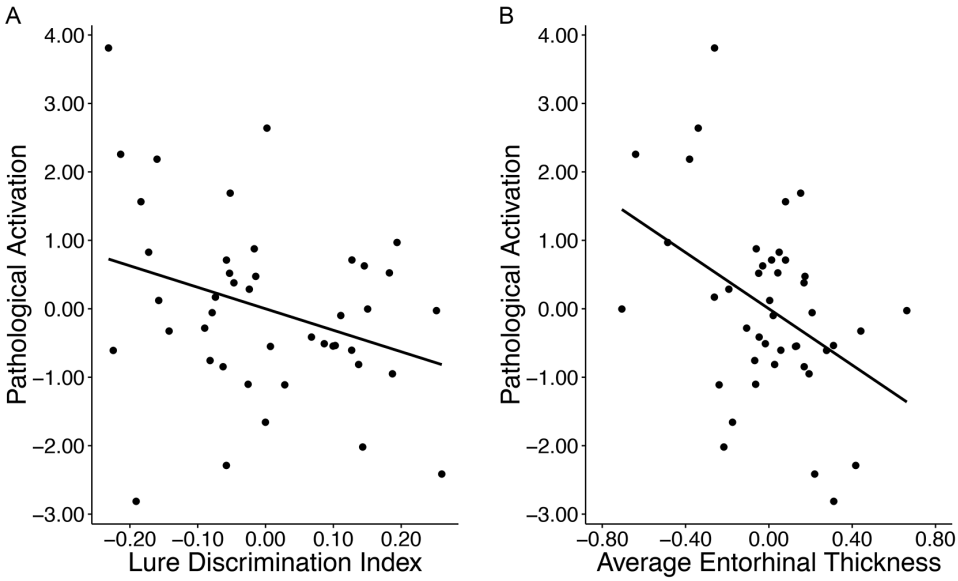

Figure 2.6. Relationship between pathological activation, memory, and cortical thickness. (A) Negative relationship between pathological activation (as defined by combining subsequent hit deactivation and subsequent false alarm activation) and lure discrimination index (r_{38} = 0.35, p = 0.05). (B) Negative relationship between pathological activation and average entorhinal cortex thickness (r_{38} = 0.44, p = 0.007). Data are residuals controlling for age, sex, and education.

Although older participants showed greater activation than younger for all 3 task conditions, we chose to examine pathological effects (as opposed to age-related effects) by combining neural measures that were uniquely susceptible to Aβ and tau. Thus, we

generated a pathological activation composite measure by combining z-transformed data for sH deactivations and sFA activations. To determine whether elevated pathological activation was detrimental to memory, average activation from the composite measure was related to the LDI. There was a significant relationship with LDI such that OA with increased pathological activation performed worse on the memory paradigm (r_{38} = 0.35, p = 0.05, Figure 2.6A). Based on extensive data linking AD pathology to MTL brain structure, we sought to explore whether hippocampal volume, and the thickness of surrounding cortical regions were also associated with pathological activation. Thinner average entorhinal cortex (r_{38} = 0.44, p = 0.007, Figure 2.6B), as well as marginally smaller hippocampal volume (r_{37} = 0.34, p = 0.07), was associated with increased pathological activation in OA. The relationship with entorhinal thickness survived a Bonferroni adjusted p-value of 0.01. Older age was additionally associated with thinner entorhinal cortex (r_{41} = 0.39, p = 0.006) and smaller hippocampal volume (r_{40} = 0.29, p = 0.04).

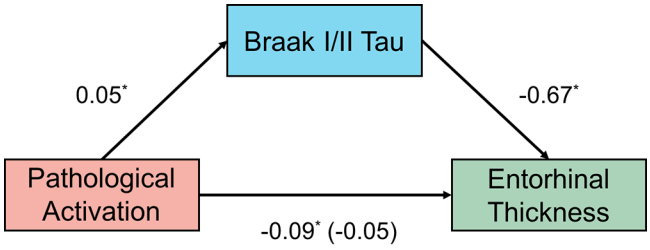

Figure 2.7. Mediation analysis between pathological activation, Braak I/II tau, and cortical thickness. Mediation analysis with pathological activation (red), mediated by Braak I/II AV-1451 standard uptake volume ratio (blue), predicting right entorhinal cortical thickness (green). Pathological activation positively predicted Braak I/II AV-1451, Braak I/II AV-1451 negatively predicted entorhinal cortical thickness, which resulted in a significant mediation. Numerical values are regression coefficients (β) from models controlling for age, sex, and education. See text for more details. $^{*}p < 0.05$.

2.5.6 Relationships between Pathology, Cortical Thickness and Pathological Activation

We sought to better understand the relationship between MTL structure, AD pathology and pathological activation; therefore, we performed a mediation analysis to better define the relationships between MTL tau, pathological activation and average entorhinal cortical thickness, as depicted in Figure 2.7. First, the total effect of pathological activation correlating with entorhinal thickness was significant in the OA with tau imaging (β = -0.09, p = 0.02). Second, as expected, pathological activation was significantly associated with Braak I/II tau (β = 0.05, p = 0.02). Third, Braak I/II tau was significantly correlated with entorhinal thickness (β = -0.67, p = 0.03). Fourth, pathological activation was no longer associated with entorhinal thickness when controlling for Braak I/II tau (β = -0.05, *n.s.*). The indirect effect was tested using a Monte Carlo simulation with 5000 simulations. The effect was measured to be -0.03 with 95% confidence intervals of (-0.08, -0.002), indicating that the indirect effect was significant. Increased pathological activation was associated with a 0.03 decrease in entorhinal thickness as mediated by Braak I/II tau pathology. A secondary analysis assessing whether Aβ also mediated the relationship between pathological activation and entorhinal cortical thickness was not significant.

2.6 Discussion

The presence of AD pathology in cognitively normal older adults may contribute to the disruption of memory function commonly observed in aging. This study explored the relationship between cognition, MTL memory network structure and function, and *in vivo* measures of tau and Aβ. We confirmed previous reports that older adults exhibit impaired lure discrimination ability, reflecting a bias towards pattern completion. We also found that tau and Aβ pathology are related to two different components of memory encoding, hits and false alarms, which we combined to describe a disruption in network function. The combined pathological activation measure was associated with both worse memory and atrophy of the MTL. Furthermore, a mediation analysis revealed that tau in the hippocampus and entorhinal cortex, explained the relationship between pathological activation and cortical thickness. These results suggest that the co-occurrence of tau and Aβ plays a critical role in the development of age-related memory decline, particularly by leading to aberrant activity throughout the hippocampal memory network and to atrophy of crucial brain structures.

2.6.1 Task Activation in Older Adult Cohorts

Increased task-induced activation has been a frequent finding in cognitively normal older adults and individuals with mild cognitive impairment (MCI). Multiple studies have reported hippocampal hyperactivity during episodic memory (Miller et al., 2008; Yassa et al., 2010b; 2011a), which may be interpreted as aberrant due to its frequent negative association with memory performance. Using the same lure discrimination paradigm, Bakker et al. (2012) reported increased hippocampal activation in amnestic MCI subjects in relation to cognitively normal older adults that was negatively associated with task performance. Although our results and numerous aging studies have reported increased hippocampal activation, others have reported decreased activation (Cabeza et al., 2004; Dennis et al., 2008) or no difference in activation (Sperling et al., 2003; Duverne et al., 2009) when compared to young controls. These disparate findings are likely related to differences in task and task difficulty, varied subject demographics, and the uncertain pathological status of participants.

2.6.2 Task Activation as a Function of Alzheimer's Pathology

Our results are in agreement with existing literature indicating that measurement of pathological proteins explains increased activation during memory encoding above the effects of chronological age. Specifically, several studies have linked elevated Aβ to altered brain function during episodic memory (Sperling et al., 2009; Mormino et al., 2012; Vannini et al., 2012a; Elman et al., 2014; Huijbers et al., 2015). Mormino et al. (2012) reported increased hippocampal activation in cognitively normal older adults with significant Aβ burden; while, Sperling et al. (2009) demonstrated that reduced task-induced deactivations were associated with elevated Aβ deposition. A recent study reported an association between increased Aβ and decreased task activation, but the hippocampus and broader MTL were not implicated (Kennedy et al., 2012). Animal models of AD have suggested that Aβ-related increased neural activity is epileptiform in

nature (Palop et al., 2007), and is in turn associated with the deposition of Aβ (Cirrito et al., 2005; Bero et al., 2011), potentially leading to a vicious cycle. Human neuroimaging data demonstrating that the anti-epileptic drug levetiracetam both reduced hippocampal activity and improved memory support this interpretation (Bakker et al., 2012).

However, some studies have suggested that increased neural activity may play a compensatory role (Miller et al., 2008). We previously reported that increased activity in parietal and occipital cortex, but not hippocampus, was associated with better memory performance in Aβ+ individuals (Elman et al., 2014). Differences in interpretation may depend to some extent on which brain regions are examined. For example, aberrant hippocampal activity may better reflect pathological changes, while activation outside of the MTL might be indicative of other processes. Regardless of the precise cause, accumulating evidence supports the view that this increased MTL activity is detrimental. Because neural activity is associated with Aβ deposition (Cirrito et al., 2005; Bero et al., 2011), it is possible that this increased hippocampal activation is driving neural activity in other cortical regions, such as the retrosplenial cortex and precuneus, that are highly connected to the hippocampus and prone to Aβ deposition. Furthermore, some have suggested a component of excitotoxic damage in the AD pathophysiological cascade (Hynd et al., 2004; Ong et al., 2013) and the observed increased activation may be related to this process, to which the hippocampus is uniquely susceptible. This idea is supported by recent evidence linking increased hippocampal activation and atrophy in AD-signature regions in cognitively normal older adults and patients with MCI (Putcha et al., 2011).

The current findings build on past studies by including measures of tau pathology along with Aβ. Decades of neuropathological investigation as well as recent clinical data support a model wherein tau accumulation becomes ubiquitous in the MTL/entorhinal cortex in normal older adults, spreads to limbic regions and neocortex with the deposition of Aβ, and strongly parallels cognition (Johnson et al., 2015; Cho et al., 2016; Ossenkoppele et al., 2016; Schöll et al., 2016; Schwarz et al., 2016). Relationships between tau deposition and hippocampal function appear reasonable in light of its topographical localization, along with evidence of its association with impaired memory (Schöll et al., 2016). For example, tau-related neurodegeneration (Spires-Jones and Hyman, 2014) and the resulting disconnection of entorhinal cortex from the hippocampus may potentiate the recurrent auto-associative fibers within the hippocampal circuitry that lead to pattern completion. In addition, there is strong evidence that tau accumulation is integral to producing aberrant neural activity in the presence of Aβ (Roberson et al., 2011). This process may be exacerbated by an age-related reduction in hippocampal inhibitory interneurons (Vela et al., 2003; Stanley and Shetty, 2004), shifting the balance of excitation and inhibition within hippocampal subfields, and leading to further aberrant activity.

2.6.3 Experimental Limitations

There are limitations to the current study. A liberal cluster threshold was utilized for all task-related activation analyses which could allow for false positives (Eklund et al., 2016). We feel that this concern is mitigated by the fact that our major findings reflect

associations between activation and other biological variables. For example, the specific regional localization of activation within the MTL is not crucial, but rather we find that molecular pathology is associated with different aspects of a larger hippocampal memory network. Previous studies implementing the same task have examined only dentate gyrus and CA3 subfield function (Bakker et al., 2008; Yassa et al., 2011a; Bakker et al., 2012). As such, they utilize hybrid functional/structural regions of interest (ROIs), which are generated by masking thresholded *F*-statistics ($p < 0.05$-0.07, $k = 10$-100 voxels) with hippocampal subfield ROIs. Their use of liberal thresholds suggests that the effects associated with this paradigm are small and may not be fully captured by strict cluster correction. However, we tried to address false positives by restricting voxelwise analyses to the hippocampus, entorhinal, perirhinal and parahippocampal cortices. By doing so, we drastically limit the number of voxels and enhance signal-to-noise. We also acknowledge that our definition of the lure discrimination index may not reflect explicit pattern separation by including lure stimuli called new. Although a response of similar or new both reflect correct responses, (since a response of new could result from judging lure stimuli to be dissimilar), it is also possible that a new response indicates inadequate encoding of the paired stimulus. We chose to include these responses in order to increase the number of trials associated with the measure; therefore, the measure may better reflect a failure of pattern completion. Additionally, not all results could be corrected for multiple comparisons using Bonferroni correction. Specifically, relationships between individual measures of task-related activation and AD pathology would be nullified. Nevertheless, the association between Aβ and reduced deactivation replicates previous reports, and the task-related activation associations with behavior and brain structure suggests their biological relevance. Finally, both PET tracers have limitations. PIB binds only to aggregated fibrillar forms of Aβ, neglecting the pathological soluble forms. Previous work demonstrates that soluble and fibrillar forms of Aβ may exist in equilibrium (Cirrito et al., 2003). However, as we have no measure of soluble Aβ, it is possible our results underestimate the strength of relationships with Aβ. Off-target binding of ^{18}F-AV-1451 in the choroid plexus also poses a problem when quantifying hippocampal tau, but this problem was addressed through partial volume correction.

2.6.4 Conclusions

In summary, our results suggest that tau and Aβ are associated with aberrant activity within the MTL during memory encoding. Given the nature of AD pathology and the onset of its accumulation, longitudinal studies across the lifespan need to be performed in order to fully understand the influence of pathology on age-related memory decline. However, these results indicate that both Aβ and tau play different but complementary roles in increasing neural activity during memory encoding, specifically in a manner that appears to be behaviorally detrimental and associated with structural brain change. These findings broaden the concept of cognitive aging to include evidence of AD-related protein aggregation as an underlying mechanism of age-related memory impairment.

Chapter 3: Neural similarity between false alarm events is associated with tau pathology in cognitively normal older adults

3.1 Overview

Chapter 2 found that the accumulation of tau pathology is associated with aberrant activity during memory encoding, but the mechanism through which episodic memory becomes impaired remains unclear. The relationship between memory encoding and retrieval has been characterized as a reinstatement of the encoding event which helps to guide the retrieval of a memory; yet, older adults often exhibit a bias towards pattern completion, which may manifest as greater neural similarity between different memory events that ultimately result in a false alarm. Using a representational similarity metric in conjunction with *in vivo* amyloid and tau PET imaging, we sought to explore neural similarity between object pairs and the impact of age and pathological burden on this relationship. In general, young adults showed greater similarity between encoding and retrieval of correct trials (i.e. hit, correct rejection), relative to incorrect trials (i.e. false alarm). Older, amyloid-negative, adults demonstrated false alarm similarity values equivalent to hits and greater than correct rejections. Increased false alarm similarity was associated with a greater proportion of false alarm events in both young controls and amyloid-negative older adults. Finally, increased tau in the hippocampus and entorhinal cortex was associated with false alarm neural similarity across older adults, but the effect was largely driven by amyloid-negative participants. These results offer a potential mechanism in which tau pathology alters the relationship between memory encoding and retrieval, leading to episodic memory impairment in cognitively normal older adults.

3.2 Introduction

Functions of the hippocampus and associated medial temporal lobe (MTL) structures involved in memory have been probed using a multitude of conceptual models and experimental paradigms. One influential approach posits that the hippocampus performs a task of pattern separation, differentiating novel from previously encountered events by orthogonalizing them into unique representations and thereby reducing interference (Marr, 1971; Treves and Rolls, 1994; O'Reilly and Norman, 2002). This model is examined using experimental approaches that present stimuli that are repeats of previously encountered stimuli, entirely new stimuli, or stimuli that are similar but subtly different from those previously presented (lures). Work in animals and humans has confirmed that unique events are defined by distinct patterns of neural activity (Leutgeb et al., 2007; Bakker et al., 2008). This is contrasted by relatively stable neural representations for identical events (Leutgeb et al., 2005; Leutgeb and Leutgeb, 2007), which has been thought to represent pattern completion, or the reactivation of neural representations when faced with partial or incomplete cues that permit identification of old items. Meanwhile, aging and the onset of Alzheimer's disease (AD) are commonly associated with changes in episodic memory. Older adults often struggle to form new memories and show a marked bias towards pattern completion when performing memory

tasks, measured experimentally as the tendency to identify a lure as a previously seen stimulus (i.e., a “false alarm”). Age-related shifts towards pattern completion have been linked to the structural degradation of perforant and limbic pathways connecting the hippocampus to surrounding cortical areas (Yassa et al., 2011b; Bennett et al., 2015). Furthermore, elevated neural activity during episodic memory tasks has been shown to be behaviorally detrimental in cognitively normal older adults and individuals with mild cognitive impairment (Yassa et al., 2011a; Bakker et al., 2012). Specifically, older adults who exhibit increased medial temporal lobe activity during memory encoding perform worse on a lure discrimination paradigm.

Both normal cognitive aging and AD are associated with the deposition of two aggregated proteins: β-amyloid (Aβ) and tau. Investigation of the in vivo pattern of deposition of these proteins in humans is possible because of PET radiopharmaceuticals that label the aggregated proteins. [^{11}C] PIB and [^{18}F] AV-1451 have been used to measure Aβ and tau in cognitively normal older adults and patients with AD (Price et al., 2005; Xia et al., 2013). Aβ deposition in the form of neuritic plaques is generally conceptualized as a crucial initiating event in the pathological cascade leading to AD (Hardy and Higgins, 1992; Jack and Holtzman, 2013). Tau deposition in the form of neurofibrillary tangles, however, occurs in the MTL in aging and is associated with memory decline even in the absence of Aβ pathology (Crary et al., 2014). Tau is thought to become widely dispersed through the brain with Aβ deposition (Tomlinson et al., 1968; Price and Morris, 1999). While both proteins are seen with normal cognitive function, widespread Aβ and tau deposition now appears to be associated with cognitive decline and dementia. The presence of Aβ is associated with aberrant task-related activation in older adults, specifically greater activation and reduced task-induced deactivations during correctly remembered events (Sperling et al., 2009; Mormino et al., 2012; Huijbers et al., 2015). Additionally, we recently reported that deposition of tau is linked to increased MTL neural activity during encoding of subsequent false alarms (Marks et al., 2017). In view of the early deposition of tau in MTL and its association with age and memory decline, there is reason to suspect that the accumulation of tau pathology leads to disconnection of the hippocampus from the larger episodic memory network, resulting in memory failure due to greater reliance on pattern completion mechanisms. Based on inferences made from animal models, if tau exacerbates a bias towards pattern completion, one might expect the patterns of neural activity associated with two unique events to be more similar when incorrectly identified as identical.

To further explore this idea, we performed a representational similarity analysis using data associated with a lure discrimination paradigm. Representational similarity has been described as a way to compare patterns of neural activity across a brain region between a given set of stimuli (Kriegeskorte et al., 2008). Past research in young adults has frequently demonstrated that neural similarity within the hippocampus is greater for events that are subsequently remembered rather than forgotten (Davis et al., 2014; Ezzyat and Davachi, 2014; Tompary et al., 2016). These studies have often used associative memory paradigms that rely on a comparison to the initial encoding event when making a decision, potentially reflecting a pattern completion mechanism. As the current paradigm allowed for not only comparisons between identical objects (hits), but

similar lure pairs, we were most interested in how incorrectly identified lure trials (false alarms) compared to hits. We hypothesized that neural similarity for hit and false alarm pairs would be equivalent in older subjects, that increased tau (measured with AV-1451 PET) in the hippocampus and entorhinal cortex would be associated with greater similarity values during false alarms, and larger similarity values would be associated with greater prevalence of false alarms.

3.3 Materials and Methods

3.3.1 Participants

Thirty-five cognitively normal older adults aged 64-93 years (27 female) and 20 young controls aged 18-30 years (13 female) were studied in a previous report (Marks et al., 2017); methods reported here for data acquisition and aspects of processing are identical to those reported previously. All participants completed a battery of neuropsychological assessments and a detailed medical interview prior to enrollment. Older adults were required to be 64 years of age or older, free of neurological and major medical illness, perform normally on neuropsychological tests (within 1.5 SD of the mean), and have participated in both PIB and AV-1451-PET imaging, in addition to the lure discrimination fMRI paradigm. Young controls did not undergo PET imaging. fMRI scans were acquired within an average of 104±102 days from PIB and 124±199 days from AV-1451 PET scans. All participants provided informed consent in accordance with the Institutional Review Boards of the University of California, Berkeley, and the Lawrence Berkeley National Laboratory (LBNL).

3.3.2 Memory Paradigm

The memory paradigm has been described previously by Marks et al. (2017). In brief, participants were shown color photographs of novel, repeated, and similar (i.e. lure) objects. Objects were displayed for 2000 ms, followed by a fixed 500 ms inter-trial interval. Participants were told to identify the objects seen as new (first), old (repeat), or similar but not identical (lure). Across six runs, participants encountered 96 repeated pairs, 96 lure pairs, and 264 novel objects, with no objects duplicated between runs. Objects were fully randomized and the distance between repeated and lure pairs was randomly varied between 10 and 40 trials.

3.3.3 PET Acquisition and Processing

PIB was synthesized at the LBNL Biomedical Isotope Facility. PIB-PET imaging was performed at LBNL using a BIOGRAPH PET/CT Truepoint 6 scanner (Siemens Medical Systems) in three-dimensional acquisition mode. Thirty-five dynamic acquisition frames were obtained over 90 minutes (4 × 15 s, 8 × 30 s, 9 × 60 s, 2 × 180 s, 10 × 300 s and 2 × 600 s) immediately following injection of 10-15mCi of PIB into an antecubital vein. An X-ray CT was obtained prior to each PIB scan. AV-1451 was synthesized at LBNL using a GE TracerLab FXN-Pro synthesis module with a modified protocol based on that supplied by Avid Radiopharmaceuticals. AV-1451 PET imaging was performed on the

same BIOGRAPH PET/CT scanner. Following the injection of 10 mCi of AV-1451, one of two acquisition schemes were acquired: 0-100 minutes of dynamic data (4 x 15 s, 8 x 30s, 9 x 60 s, 2 x 180 s and 16 x 300 s frames), followed by 120-150 minutes (6 x 300 s frames, n = 18), or 75-115 minutes (8 x 300 s frames, n = 17). A CT scan was performed before the start of each emission acquisition. PIB and AV-1451 data were reconstructed using an ordered subset expectation maximization algorithm with weighted attenuation and smoothed with a 4 mm Gaussian kernel with scatter correction.

PET data were processed using the SPM12 software package (RRID:SCR_007037). PIB-PET data were realigned and frames corresponding to the first 20 minutes of acquisition were averaged and used to guide coregistration with the participant's structural MRI. The coregistration matrix was applied to realigned frames and data were resliced to MRI space. Distribution volume ratio (DVR) images of PIB-PET data 35-90 minutes post-injection were created using Logan graphical analysis and a FreeSurfer derived grey cerebellum reference region (Logan, 2000). Global PIB DVR values were calculated for each participant, defined as the mean DVR within regions of interest (ROI) in frontal, parietal, temporal and cingulate cortices. A PIB DVR value greater than 1.07 was used as a cutoff for categorizing older adults as Aβ-positive (Villeneuve et al., 2015).

AV-1451-PET data were realigned and the mean of all frames was used to coregister data to the participant's structural MRI. Standard uptake value (SUV) images representing data 80-100 minutes post-injection were created and normalized by a grey cerebellum reference region to generate native space SUV ratio (SUVR) images. SUVR images were partial volume corrected using the Rousset approach (Rousset et al., 1998). Volume-weighted mean SUVR values within hippocampus and entorhinal cortex, approximating Braak stage I/II, were calculated using a previously described method (Schöll et al., 2016).

3.3.4 MRI Acquisition and Processing

High-resolution fMRI was performed at the Henry H. Wheeler Jr. Brain Imaging Center (BIC) on a 3T TIM/Trio scanner (Siemens Medical Systems) using a 32-channel head coil. Each of the six functional runs utilized a T2*-weighted echo-planar imaging sequence (TR = 1500 ms; TE = 34 ms; flip angle = 70°; matrix = 132 x 132; FOV = 200; voxel size = 1.5 x 1.5 x 1.5 mm; duration = 5 min). Nineteen slices oriented parallel to the primary axis of the hippocampus were acquired in interleaved order, covering the entirety of the MTL. A parallel imaging reduction factor of 2 was used to reduce acquisition time and minimize distortion due to magnetic susceptibilities near the temporal lobes. A T1-weighted volumetric magnetization prepared rapid gradient echo (MPRAGE; TR = 2300 ms; TE = 2.98 ms; matrix = 256 x 256; FOV = 256; sagittal plane; voxel size = 1 x 1 x 1 mm; 160 slices) was collected and used during coregistration of functional data. An MPRAGE (TR = 2,110 ms; TE = 3.58 ms; matrix = 256 × 256; FOV = 256; sagittal plane; voxel size = 1 × 1 × 1 mm; 160 slices) was collected at LBNL on a 1.5T Magnetom Avanto (Siemens Medical Systems) and used only for PET coregistration and quantification purposes. Structural MRI data were processed using FreeSurfer version 5.3 (RRID:SCR_001847) to define native space ROIs for each participant (Dale et al., 1999;

Fischl et al., 2001; 2002; Ségonne et al., 2004). FreeSurfer ROIs were used to quantify PIB DVR and AV-1451 SUVR values.

3.3.5 fMRI Processing and Analysis

fMRI data were processed and analyzed using a combination of Advanced Normalization Tools (RRID:SCR_004757) and SPM12. For a given run, images were realigned to the first volume and smoothed with a 5 mm Gaussian kernel. Motion vectors were created and used to identify significant motion spikes (greater than 2 mm displacement, plus and minus one TR). A mean fMRI image was created, bias corrected, and thresholded to exclude surrounding non-brain tissue and skull. The resulting image was used in a two-step spatial normalization process, resulting in fMRI data in MNI space.

Individual runs were modeled using FSL's FEAT version 6.0 (RRID:SCR_002823). Trials were categorized into eight bins. Four of these represented activity upon the first presentation of the stimuli: (1) novel objects (stimuli presented only once), (2) subsequent hits, (3) subsequent correct rejections, and (4) subsequent false alarms. Three represented activity upon presentation of the paired stimuli: (5) hits (repeat presentation correctly identified as old), (6) correct rejections (lure presentations correctly identified as similar), (7) false alarms (lure presentations incorrectly identified as old), with an 8^{th} category of errors and omissions. Data were convolved with a double gamma hemodynamic response function, and each bin, their corresponding temporal derivatives, six rigid body motion parameters, and outlier volumes (those with excessive motion) were entered in a general linear model to predict fMRI signal. The resulting contrasts reflect activity for a given task-related bin relative to the non-zero, novel object baseline condition. Second-level contrasts were created for each participant by combining all six runs using a one-sample *t*-test with fixed effects.

3.3.6 Representational Similarity Analysis

Using output from the univariate activation models (described above), we first extracted beta values from a large medial temporal lobe ROI, comprising the hippocampus and perirhinal, entorhinal, and parahippocampal cortices, for the first (encoding) and second (retrieval) presentation of object pairs categorized as hits, correct rejections and false alarms. The large ROI was manually segmented in MNI space following previously established guidelines (Insausti et al., 1998; Pruessner et al., 2002; Duvernoy, 2005). The encoding and retrieval beta values were z-scored across all voxels in the ROI, transformed into vectors and correlated with one another. The resulting correlation coefficients (Pearson's *r*) were Fisher transformed and used as a measure of neural similarity. Higher values are taken to indicate that the pattern of neural activity for encoding and retrieval trials are similar for a given condition.

3.3.7 Statistical Analyses

Statistical analyses and plots were performed using R version 3.2.3 (RRID:SCR_001905). Differences between and within groups were assessed using *t*-test

and analysis of variance (ANOVA) with post-hoc Tukey test. Multiple linear regression, controlling for demographic variables, was used to assess the relationships between representational similarity, task performance, and tau pathology. Mediation analysis were performed using the 'mediation' package in R.

3.4 Results

3.4.1 Memory Performance

To quantify performance on hit and false alarm trials, the number of repeated objects called 'old' and lure objects called 'old' were calculated, respectively. To assess correct rejections, the number of lure objects called 'similar' minus the number of novel objects called 'similar' was calculated. The removal of novel objects called 'similar' ensures the lack of an inherent bias towards responding 'similar' for all objects. Young controls performed significantly better than older adults on both hit ($t_{(53)}$ = 3.64, P < 0.001) and correct rejection trials ($t_{(53)}$ = 6.36, P < 0.001). However, older adults made significantly more false alarms than young controls ($t_{(53)}$ = 2.85, P = 0.006). Prior to assessing representational similarity within older adults, we dichotomized older participants by Aβ-status to better isolate the influence of tau on neural function. This resulted in 19 PIB- and 16 PIB+ individuals. Performance did not differ between PIB groups for any trial type.

3.4.2 Representational Similarity by Group

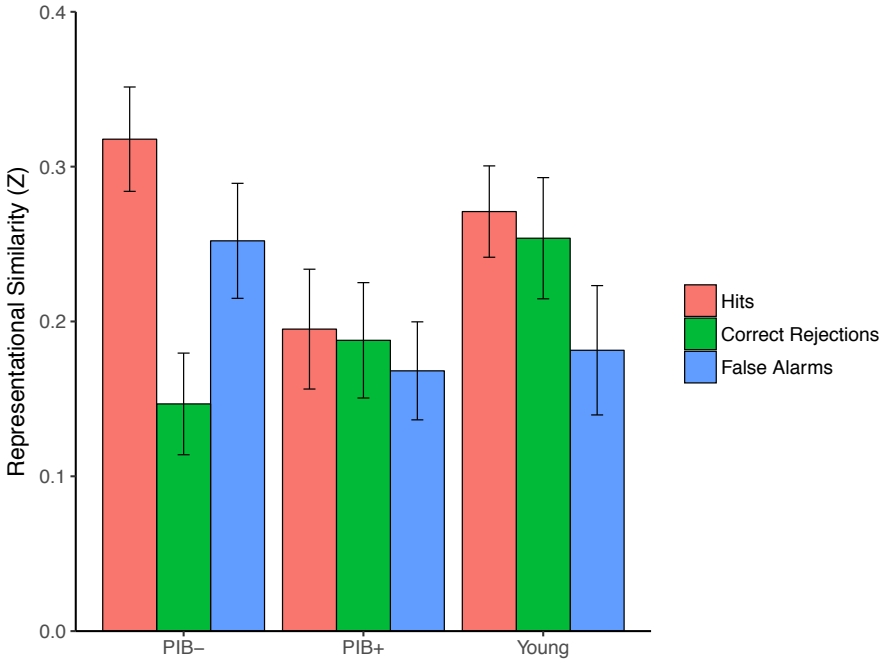

Figure 3.1. Neural similarity split by group and trial type. A trial type by group ANOVA revealed a main effect of trial type. Post-hoc analyses revealed that neural similarity for hits was greater than correct rejections and false alarms. Data presented as means ± standard error.

We first wanted to assess how representational similarity differed by trial type across groups. A 3x3 ANOVA demonstrated a significant main effect of trial type ($F_{(2,104)} = 3.52$, $P = 0.03$; Figure 3.1), with the trial type by group interaction approaching significance ($F_{(4,104)} = 1.74$, $P = 0.14$). A post-hoc Tukey test revealed that similarity for hits, across groups, was greater than correct rejections and false alarms. To better understand the relationship between similarity and trial type, we next explored differences between trial types within each group. Within young controls, similarity for hits was marginally greater than false alarms ($t_{(18)} = 1.75$, $P = 0.09$). No other differences were observed in this group. Within PIB- older adults, similarity for hits was greater than correct rejections ($t_{(17)} = 3.26$, $P = 0.002$). Neural similarity for false alarms was also greater than correct rejections but only at a trend level ($t_{(17)} = 1.57$, $P = 0.12$). We did not observe any differences between trial types within PIB+ older adults, but their values were generally reduced compared to the PIB- and young control groups.

3.4.3 Relationship between Representational Similarity and Performance

Although neural similarity has previously been associated with successful memory, the differences between false alarms and correct rejections in PIB- older adults suggests that similarity during false alarms could reflect a pattern completion mechanism that adversely affects performance during lure discrimination. As such, we sought to relate performance on the memory paradigm with similarity values associated with each trial type. Young controls showed no relationship between performance on hits or correct rejections and their respective similarity values.

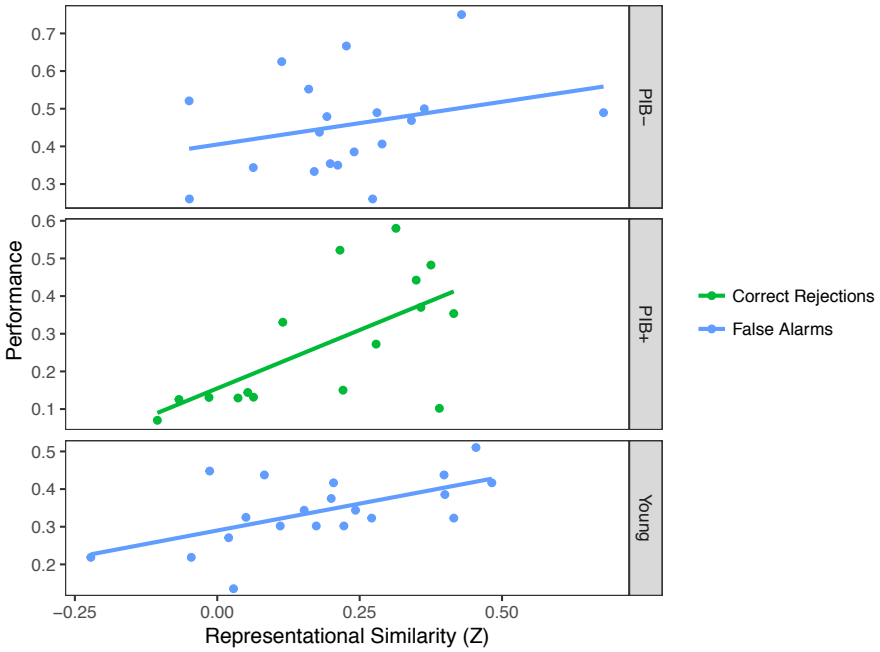

Figure 3.2. Relationship between neural similarity and task performance. In young adults (r = 0.45, P = 0.02) and PIB- older adults (r = 0.21, P = 0.08): positive relationship between false alarm similarity and the proportion of lures incorrectly identified as "old." In PIB+ older adults (r = 0.79, P = 0.005): positive relationship between correct rejection similarity and proportion of correctly identified lures. Data are residuals controlling for age, sex, and education.

However, there was a relationship between proportions of false alarms and similarity such that larger similarity values were associated with more false alarms (β = 0.27, r = 0.45, *P* = 0.02; Figure 3.2). PIB- older adults showed a similar relationship (β = 0.44, r = 0.21, *P* = 0.08). Interestingly, in PIB+ older adults, better memory for lure pairs was associated with increased neural similarity during correct rejections (β = 0.59, r = 0.79, *P* = 0.005), but no relationships were found with hits or false alarms.

3.4.4 Relationship between Representational Similarity and Tau Pathology

As neural similarity during false alarms appears to negatively impact memory performance, we sought to understand whether underlying tau pathology in the medial temporal lobes might play a role in the observed impairment. Across all older adults, there was a significant relationship between tau in the hippocampus and entorhinal cortex and false alarm similarity. Older adults with increased tau pathology demonstrated greater false alarm similarity (β = 0.34, r = 0.49, *P* = 0.02); however, this relationship appeared to be driven by PIB- older adults (β = 0.52, r = 0.73, *P* = 0.004), as PIB+ showed no significant relationship between tau and false alarm similarity when assessed independently (β = -0.02, *P* = 0.95; Figure 3.3). There was no significant interaction between groups.

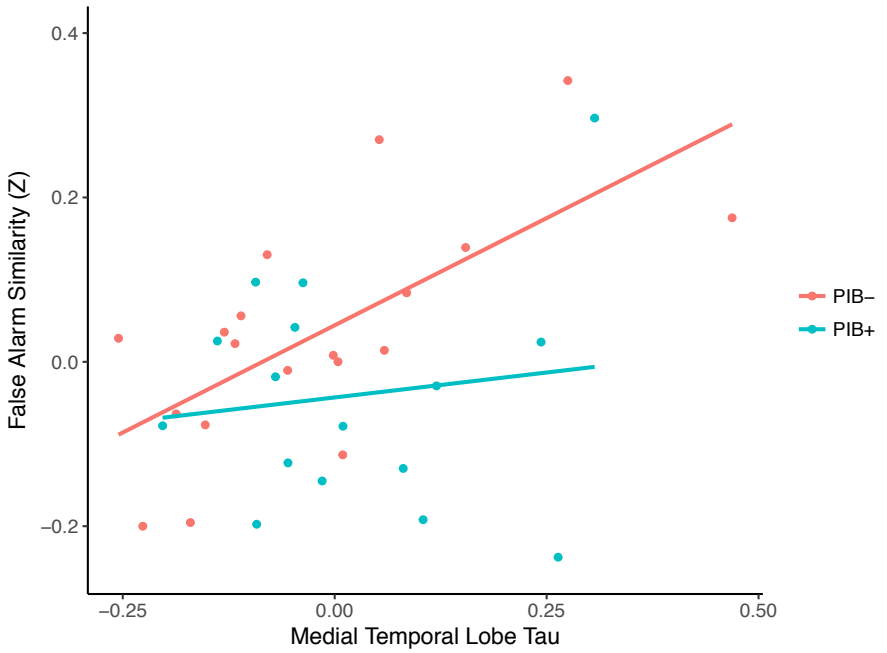

Figure 3.3. Relationship between neural similarity and tau. Positive relationship between false alarm similarity and medial temporal lobe tau (as measured by AV-1451 in entorhinal cortex and hippocampus). Significant relationship was only observed in PIB- older adults (r = 0.73, P = 0.004). Data are residuals controlling for age and sex.

Since false alarm similarity was associated with both tau pathology and task performance, we sought to better understand this relationship by performing a formal mediation analysis. We observed that false alarm similarity in older adults partially mediated the relationship between medial temporal lobe tau pathology and incidence of false alarms

during lure discrimination. The effect was assessed using quasi-Bayesian approximation with 5000 simulations and measured to be 0.16 with 95% confidence intervals (0.01, 0.37) at $P = 0.03$. In other words, increased tau pathology was associated with a 0.16 increase in false alarms as mediated by neural similarity. The mediation effect remained even after controlling for Aβ-status.

3.5 Discussion

The accumulation of tau pathology has previously been linked to cognitive decline in older adults. The current study sought to understand a mechanism through which tau pathology impairs memory performance by using representational similarity to explore neural patterns during the encoding and retrieval of object pairs. Similarity values in young controls were largely consistent with previous reports, as correctly remembered trials showed greater similarity than false alarms. In older adults, similarity vales were drastically different, particularly in PIB- participants who demonstrated false alarm similarity values equivalent to hits and greater than correct rejections. The observed increased false alarm similarity appeared to be behaviorally detrimental as a higher prevalence of false alarms was seen in both PIB- older adults and young controls with large similarity values. Furthermore, increased neural similarity during false alarms was associated with elevated tau in the hippocampus and entorhinal cortex in older adults; however, the effect appeared to be driven by PIB- participants. A mediation analysis revealed that false alarm similarity partially explained the relationship between tau pathology and the incidence of false alarms, irrespective of Aβ status. These results provide evidence for a way in which the accumulation of tau pathology in the medial temporal lobes leads to changes in episodic memory ability in cognitively normal older adults without Aβ.

It has been suggested that increased similarity reflects a neural reinstatement of the encoding event during retrieval (van den Honert et al., 2016). As an example, we might expect the pattern of neural activity to be similar for the first and second presentation of an identical object pair if it is encoded as a singular event. However, since the current study employed not only identical pairs, but similar lure pairs, the interpretation of what similarity during lure trials represents is less clear. Previous work has demonstrated that older adults often incorrectly identify lures as old repetitions, instead of unique events (Yassa et al., 2011a). This has commonly been described as pattern completion, which leads to false alarms that closely mirror the behavior of successfully remembered identical pairs. The relative equivalence of hit and false alarm similarity values in older adults and young controls suggests that the medial temporal lobes represent the two behaviors similarly.

Until now, limited work has been done to explore how neural similarity differs between older adults and young controls. This is an important distinction to make as even cognitively normal older adults begin to accumulate tau pathology in midlife that is associated with changes in cognition, particularly memory. Previous work has demonstrated that both Aβ and tau are associated with aberrant neural activity during memory tasks and at rest (Sperling et al., 2009; Mormino et al., 2012; Marks et al., 2017),

and tau is closely linked to Alzheimer's disease symptoms (Arriagada et al., 1992; van Rossum et al., 2012). Considering its topography within the medial temporal lobes, it is reasonable to conclude that tau-related neurodegeneration (Spires-Jones and Hyman, 2014) disconnects the hippocampus from the larger episodic memory system, potentiating the recurrent fiber pathways that lead to pattern completion (Amaral and Lavenex, 2006). The same pattern completion mechanism observed in young controls is likely exacerbated by the accumulation of tau in older adults. This is further evident when examining the relationships between tau, false alarm similarity and task performance. Even though our interpretation relies heavily on the role of the hippocampus in the encoding of object stimuli, the ROI used to calculate representational similarity also included perirhinal cortex. A perirhinal memory system has been proposed which is active during object recognition (Brown and Aggleton, 2001; Aggleton and Brown, 2006; Ranganath and Ritchey, 2012), but is generally more associated with familiarity or 'knowing,' rather than explicitly remembering (see (Yonelinas, 2002; Yonelinas et al., 2010) for a review). As such, the observed similarity during false alarms likely reflects a combination of tau-related bias towards pattern completion and perirhinal familiarity signals.

Although our hypothesis focused on the role of tau pathology, Aβ may nevertheless be important. The relationship between correct rejection similarity and task performance in PIB+ individuals is interesting. We argue that increased similarity during false alarms is detrimental to performance in PIB- older adults and young controls; however, it may be that the relationship with correct rejections represents a compensatory response to the accumulation of both Aβ and tau pathology. We previously reported that increased neural activity in parietal and occipital areas was associated with more detailed memory in PIB+ older adults (Elman et al., 2014). It is possible then that more similar neural representations of lure objects resulted from compensatory activity in PIB+ older adults to better cope with the adverse effects of increased pathology.

However, this interpretation does not explain the reduced correct rejection similarity values in PIB- older adults. One explanation for this disparity may have to do with the sparseness of univariate activation during encoding of correct rejections that we previously reported within this cohort (Marks et al., 2017). We found few clusters of activation that survived a liberal threshold when comparing activity across older adults. Additionally, we found little overlap in the patterns of univariate correct rejection activation between older adults and young controls. This suggests that (1) there may not be a unique representation of neural lure discrimination in older adults, and (2) older adults are likely using different mechanisms to correctly identify lures than young controls. Unfortunately, we are unable to elucidate these explicit mechanisms which may help us further explain the observed age-related differences in correct rejection similarity. With larger sample sizes, we likely could have made stronger conclusions about the relationship between pathology and neural similarity within older adults, but despite this limitation, we believe our results offer a novel mechanism through which the accumulation of Alzheimer's pathology leads to memory impairment in cognitively normal older adults.

Chapter 4: Conclusion

4.1 Overview

In this dissertation, I have demonstrated that cognitively normal older adults exhibit a behavioral shift from pattern separation towards pattern completion that is associated with aberrant neural activity in the hippocampus and MTL; and, the degree of aberrant activity is associated with elevated levels of pathology (Chapter 2). Furthermore, I provided evidence for a tau-specific mechanism that alters the relationship between memory encoding and retrieval, leading to impaired episodic memory (Chapter 3). These results indicate that, to an extent, age-related memory impairment and functional alterations can be attributed to the interaction of Aβ and tau pathology. In particular, it appears that tau is uniquely driving changes locally within the MTL.

4.2 Remaining Questions

Despite these findings, the research raises a number of questions that warrant further discussion. First, the results make assumptions based on the underlying neural function during an explicit memory paradigm. In other words, they do not consider the baseline level of activity in older adults. It is reasonable to conclude that if aberrant neural activity during a task represents a measure of dysfunction, the hippocampus may also be impaired at rest. In a subset of the older adult cohort, I attempted to address this question using a PET derived measure of glucose metabolism. Unfortunately, no relationship was observed between resting hippocampal glucose metabolism and pathological activation, Aβ or tau. I hesitate to make any conclusions from this null result, but it may suggest that Aβ and tau hinder the flow of information from the entorhinal cortex to hippocampus during effortful work, thus explaining the task-dependent nature of the results. Most published data in aging do not suggest clear baseline differences in hippocampal metabolism with advancing age; if anything, the trend is for age-related metabolic reductions. As such, the task-related activity does not appear to reflect baseline levels of metabolism.

Second, the results indicate that the accumulation of tau pathology plays a specific role in age-related memory decline, whereas the role of Aβ is less defined. I have shown in Chapter 2, as well as previous work from the lab, that Aβ is associated with aberrant neural activity, but the relationship is not necessarily hippocampus-specific. A simple explanation might be that Aβ has a more global effect, due to its relative sparing of MTL structures. Instead, it likely alters the function of intermediary brain regions that have reciprocal connections to the hippocampus. One way to address this would be to investigate the relationship between Aβ and a measure of functional connectivity. Specifically, resting functional connectivity between retrosplenial cortex (an area of high Aβ burden) and the hippocampus. These data were collected along with task-activation measures, but I was not able to find any associations between Aβ and connectivity, or between connectivity and pathological activation. It is possible that this method of functional connectivity is not suitable. Connectivity was assessed at rest, but the previous chapters and preliminary metabolic analysis indicate that pathological activation is task-

dependent. As such, a measure of task-based connectivity may have been better suited to assess the relationship with Aβ. In fact, previous work has demonstrated that Aβ is associated with decreased task-dependent connectivity during a visual memory encoding task (Oh and Jagust, 2013). However, the limited field of view at which the task data were acquired prohibited such an analysis.

Third, the results encompass other cortical structures within the MTL in addition to the hippocampus; yet, previous work has indicated that aberrant activity, with respect to measures of pattern separation, is localized in the DG/CA3. These data proved difficult to work with due to the wide variability in performance in the older adult cohort. As such, the most pronounced effects were only seen when collapsing across subjects within a large MTL region of interest. A post-hoc analysis exploring individual subfields revealed that DG/CA3 did exhibit increased task-activation, but no statistical difference was observed between older and young adults due to the large variance in the measures. It should be noted that previous fMRI studies in humans have reported small effects when identifying subfield differences, so it is not unrealistic to report a null result. Currently, the lab is exploring ways to implement new imaging sequences, such as multiband echo planar imaging, to increase spatial resolution in order to make more informed assessments of individual hippocampal subfield differences.

4.3 Future Directions

As such, a number of future directions should be considered. Building off the current results, two follow-up studies are underway in the lab that further explore the relationship between hippocampal function and pathology. The first aims to identify the contributions of anterior and posterior hippocampal memory systems to pattern separation during an 'objects in scenes' discrimination task. This research will help to assess regional specificity of age-related decline within the hippocampus proper, something which I was not able to accomplish. It will also provide an interesting avenue to explore whether the influence of pathology is global in nature or unique to specific subsystems of the hippocampus. The other aims to explore the impact of emotional stimuli on pattern separation mechanisms, particularly during memory retrieval. The current research relied on common, everyday objects as stimuli which may not have been salient in older adults' lives. It will be interesting to see whether emotional stimuli result in better memory performance and how these stimuli are represented in the hippocampus. Additionally, there is a body of work that suggests emotional memory is impaired in early AD, so any relationships with pathology in cognitively normal older adults might help to elucidate these past findings. Preliminary data for both are limited.

Another interesting line of research would be to consider these results from the framework of neuromodulation. Neural noise during information processing has been associated with decreased dopaminergic neuromodulation in aging (see (Li et al., 2001) for a review). The lab can quantify dopamine synthesis using PET, and it would be interesting to explore how neural activity during a memory paradigm relates to this measure. Individuals with impaired dopamine synthesis may also be the ones exhibiting the most aberrant activity. This study could also provide insight into a possible compensatory mechanism that allows

older adults to maintain adequate levels of performance when faced with increased pathology.

Finally, although beyond the scope of the lab, it would be interesting to explore pattern separation mechanisms in a transgenic mouse model of AD. Neural activity could be recorded directly from neurons in hippocampal subfields while three different lines of mice (Aβ+/tau-, Aβ-/tau+, Aβ+/tau+) explored novel environments. This paradigm could possibly isolate the individual effects Aβ and tau have on age-related neural rigidity. Additionally, more elegant measures of connectivity could be quantified that assess the relationship between the location of pathology and its downstream effects on neighboring brain structures crucial to memory.

References

Aggleton JP, Brown MW (2006) Interleaving brain systems for episodic and recognition memory. Trends Cogn Sci 10:455–463.

Amaral D, Lavenex P (2006) Hippocampal neuroanatomy. In: The hippocampus book (Andersen P, Morris R, Amaral D, Bliss T, OKeefe J, eds), pp 37–114. Oxford University Press.

Arriagada PV, Growdon JH, Hedley-Whyte ET, Hyman BT (1992) Neurofibrillary tangles but not senile plaques parallel duration and severity of Alzheimer's disease. Neurology 42:631–639.

Bakker A, Kirwan CB, Miller M, Stark CEL (2008) Pattern separation in the human hippocampal CA3 and dentate gyrus. Science 319:1640–1642.

Bakker A, Krauss GL, Albert MS, Speck CL, Jones LR, Stark CE, Yassa MA, Bassett SS, Shelton AL, Gallagher M (2012) Reduction of hippocampal hyperactivity improves cognition in amnestic mild cognitive impairment. Neuron 74:467–474.

Barnes CA, McNaughton BL, Mizumori SJ, Leonard BW, Lin LH (1990) Comparison of spatial and temporal characteristics of neuronal activity in sequential stages of hippocampal processing. Prog Brain Res 83:287–300.

Barnes CA, Rao G, Houston FP (2000) LTP induction threshold change in old rats at the perforant path--granule cell synapse. Neurobiol Aging 21:613–620.

Barnes CA, Treves A, Rao G, Shen J (1994) Electrophysiological markers of cognitive aging: region specificity and computational consequences. Seminars in Neuroscience 6:359–367.

Bennett DA, Schneider JA, Arvanitakis Z, Kelly JF, Aggarwal NT, Shah RC, Wilson RS (2006) Neuropathology of older persons without cognitive impairment from two community-based studies. Neurology 66:1837–1844.

Bennett IJ, Huffman DJ, Stark CEL (2015) Limbic tract integrity contributes to pattern separation performance across the lifespan. Cereb Cortex 25:2988–2999.

Bennett IJ, Stark CEL (2016) Mnemonic discrimination relates to perforant path integrity: An ultra-high resolution diffusion tensor imaging study. Neurobiology of Learning and Memory 129:107–112.

Bero AW, Yan P, Roh JH, Cirrito JR, Stewart FR, Raichle ME, Lee J-M, Holtzman DM (2011) Neuronal activity regulates the regional vulnerability to amyloid-β deposition. Nat Neurosci 14:750–756.

Braak H, Braak E (1991) Neuropathological stageing of Alzheimer-related changes. Acta Neuropathol 82:239–259.

Braak H, Braak E (1997) Frequency of stages of Alzheimer-related lesions in different age categories. Neurobiol Aging 18:351–357.

Brown MW, Aggleton JP (2001) Recognition memory: what are the roles of the perirhinal cortex and hippocampus? Nat Rev Neurosci 2:51–61.

Busche MA, Chen X, Henning HA, Reichwald J, Staufenbiel M, Sakmann B, Konnerth A (2012) Critical role of soluble amyloid-β for early hippocampal hyperactivity in a mouse model of Alzheimer's disease. Proc Natl Acad Sci USA 109:8740–8745.

Busche MA, Eichhoff G, Adelsberger H, Abramowski D (2008) Clusters of hyperactive neurons near amyloid plaques in a mouse model of Alzheimer's disease. Science 321:1686–1689.

Cabeza R (2002) Hemispheric asymmetry reduction in older adults: The HAROLD model. Psychology and Aging 17:85–100.

Cabeza R, Daselaar SM, Dolcos F, Prince SE, Budde M, Nyberg L (2004) Task-independent and task-specific age effects on brain activity during working memory, visual attention and episodic retrieval. Cereb Cortex 14:364–375.

Chabrier MA, Blurton-Jones M, Agazaryan AA, Nerhus JL, Martinez-Coria H, LaFerla FM (2012) Soluble Aβ promotes wild-type tau pathology in vivo. J Neurosci 32:17345–17350.

Cho H, Choi JY, Hwang MS, Kim YJ, Lee HM, Lee HS, Lee JH, Ryu YH, Lee MS, Lyoo CH (2016) In vivo cortical spreading pattern of tau and amyloid in the Alzheimer disease spectrum. Ann Neurol 80:247–258.

Chouinard ML, Gallagher M, Yasuda RP, Wolfe BB, McKinney M (1995) Hippocampal muscarinic receptor function in spatial learning-impaired aged rats. Neurobiol Aging 16:955–963.

Cirrito JR, May PC, O'Dell MA, Taylor JW, Parsadanian M, Cramer JW, Audia JE, Nissen JS, Bales KR, Paul SM, DeMattos RB, Holtzman DM (2003) In vivo assessment of brain interstitial fluid with microdialysis reveals plaque-associated changes in amyloid-beta metabolism and half-life. J Neurosci 23:8844–8853.

Cirrito JR, Yamada KA, Finn MB, Sloviter RS, Bales KR, May PC, Schoepp DD, Paul SM, Mennerick S, Holtzman DM (2005) Synaptic activity regulates interstitial fluid amyloid-β levels in vivo. Neuron 48:913–922.

Cleary JP, Walsh DM, Hofmeister JJ, Shankar GM, Kuskowski MA, Selkoe DJ, Ashe KH (2004) Natural oligomers of the amyloid-β protein specifically disrupt cognitive function. Nat Neurosci 8:79–84.

Crary JF et al. (2014) Primary age-related tauopathy (PART): a common pathology associated with human aging. Acta Neuropathol 128:755–766.

Dale AM, Fischl B, Sereno MI (1999) Cortical surface-based analysis. I. Segmentation and surface reconstruction. NeuroImage 9:179–194.

Davis T, Xue G, Love BC, Preston AR, Poldrack RA (2014) Global neural pattern similarity as a common basis for categorization and recognition memory. J Neurosci 34:7472–7484.

Dennis NA, Hayes SM, Prince SE, Madden DJ, Huettel SA, Cabeza R (2008) Effects of aging on the neural correlates of successful item and source memory encoding. J Exp Psychol Learn Mem Cogn 34:791–808.

Dickerson BC, Salat DH, Greve DN, Chua EF (2005) Increased hippocampal activation in mild cognitive impairment compared to normal aging and AD. Neurology 65:404–411.

Duverne S, Motamedinia S, Rugg MD (2009) The relationship between aging, performance, and the neural correlates of successful memory encoding. Cereb Cortex 19:733–744.

Duvernoy HM (2005) The human hippocampus. Berlin: Springer.

Eklund A, Nichols TE, Knutsson H (2016) Cluster failure: why fMRI inferences for spatial extent have inflated false-positive rates. Proc Natl Acad Sci USA 113:7900–7905.

Elman JA, Oh H, Madison CM, Baker SL, Vogel JW, Marks SM, Crowley S, O'Neil JP, Jagust WJ (2014) Neural compensation in older people with brain amyloid-β deposition. Nat Neurosci 17:1316–1318.

Ezzyat Y, Davachi L (2014) Similarity breeds proximity: pattern similarity within and across contexts is related to later mnemonic judgments of temporal proximity. Neuron 81:1179–1189.

Fischl B, Liu A, Dale AM (2001) Automated manifold surgery: constructing geometrically accurate and topologically correct models of the human cerebral cortex. IEEE Trans Med Imaging 20:70–80.

Fischl B, Salat DH, Busa E, Albert M, Dieterich M, Haselgrove C, van der Kouwe A, Killiany R, Kennedy D, Klaveness S, Montillo A, Makris N, Rosen B, Dale AM (2002) Whole brain segmentation: automated labeling of neuroanatomical structures in the human brain. Neuron 33:341–355.

Fonov VS, Evans AC, McKinstry RC, Almli CR, Collins DL (2009) Unbiased nonlinear average age-appropriate brain templates from birth to adulthood. Hum Brain Mapp 47:S102.

Geinisman Y, Detoledo-Morrell L, Morrell F, Persina IS, Rossi M (1992) Age-related loss of axospinous synapses formed by two afferent systems in the rat dentate gyrus as revealed by the unbiased stereological dissector technique. Hippocampus

2:437–444.

Giannakopoulos P, Herrmann FR, Bussiere T, Bouras C, Kövari E, Perl DP, Morrison JH, Gold G, Hof PR (2003) Tangle and neuron numbers, but not amyloid load, predict cognitive status in Alzheimer's disease. Neurology 60:1495–1500.

Gomez-Isla T, Hollister R, West H, Mui S, Growdon JH, Petersen RC, Parisi JE, Hyman BT (1997) Neuronal loss correlates with but exceeds neurofibrillary tangles in Alzheimer's disease. Ann Neurol 41:17–24.

Götz J, Chen F, van Dorpe J, Nitsch RM (2001) Formation of neurofibrillary tangles in P301l tau transgenic mice induced by Abeta 42 fibrils. Science 293:1491–1495.

Hardy J (2009) The amyloid hypothesis for Alzheimer's disease: a critical reappraisal. J Neurochem 110:1129–1134.

Hardy JA, Higgins GA (1992) Alzheimer's disease: the amyloid cascade hypothesis. Science 256:184–185.

Harkany T, Penke B, Luiten PG (2000) β-Amyloid excitotoxicity in rat magnocellular nucleus basalis. Effect of cortical deafferentation on cerebral blood flow regulation and implications for Alzheimer's disease. Annals of the New York Academy of Sciences 903:374–386.

Hedden T, Gabrieli JDE (2004) Insights into the ageing mind: a view from cognitive neuroscience. Nat Rev Neurosci 5:87–96.

Huijbers W, Mormino EC, Schultz AP, Wigman S, Ward AM, Larvie M, Amariglio RE, Marshall GA, Rentz DM, Johnson KA, Sperling RA (2015) Amyloid-β deposition in mild cognitive impairment is associated with increased hippocampal activity, atrophy and clinical progression. Brain 138:1023–1035.

Huijbers W, Mormino EC, Wigman SE, Ward AM, Vannini P, McLaren DG, Becker JA, Schultz AP, Hedden T, Johnson KA, Sperling RA (2014) Amyloid deposition is linked to aberrant entorhinal activity among cognitively normal older adults. J Neurosci 34:5200–5210.

Hynd MR, Scott HL, Dodd PR (2004) Glutamate-mediated excitotoxicity and neurodegeneration in Alzheimer's disease. Neurochem Int 45:583–595.

Insausti R, Juottonen K, Soininen H, Insausti AM, Partanen K, Vainio P, Laakso MP, Pitkänen A (1998) MR volumetric analysis of the human entorhinal, perirhinal, and temporopolar cortices. Am J Neuroradiol 19:659–671.

Jack CR, Holtzman DM (2013) Biomarker modeling of Alzheimer's disease. Neuron 80:1347–1358.

Jernigan TL, Archibald SL, Berhow MT, Sowell ER, Foster DS, Hesselink JR (1991)

Cerebral structure on MRI, part I: localization of age-related changes. Biol Psychiatry 29:55–67.

Johnson KA et al. (2015) Tau positron emission tomographic imaging in aging and early Alzheimer disease. Ann Neurol 79:110–119.

Kennedy KM, Rodrigue KM, Devous MD Sr, Hebrank AC, Bischof GN, Park DC (2012) Effects of beta-amyloid accumulation on neural function during encoding across the adult lifespan. NeuroImage 62:1–8.

Khlistunova I, Biernat J, Wang Y, Pickhardt M, Bergen von M, Gazova Z, Mandelkow E, Mandelkow E-M (2006) Inducible expression of tau repeat domain in cell models of tauopathy: aggregation is toxic to cells but can be reversed by inhibitor drugs. J Biol Chem 281:1205–1214.

Kriegeskorte N, Mur M, Ruff DA, Kiani R, Bodurka J, Esteky H, Tanaka K, Bandettini PA (2008) Matching categorical object representations in inferior temporal cortex of man and monkey. Neuron 60:1126–1141.

Laakso MP, Partanen K, Riekkinen P, Lehtovirta M, Helkala EL, Hallikainen M, Hanninen T, Vainio P, Soininen H (1996) Hippocampal volumes in Alzheimer“s disease, Parkinson”s disease with and without dementia, and in vascular dementia: an MRI study. Neurology 46:678–681.

Leutgeb JK, Leutgeb S, Moser M-B, Moser EI (2007) Pattern separation in the dentate gyrus and CA3 of the hippocampus. Science 315:961–966.

Leutgeb JK, Leutgeb S, Treves A, Meyer R, Barnes CA, McNaughton BL, Moser M-B, Moser EI (2005) Progressive transformation of hippocampal neuronal representations in “morphed” environments. Neuron 48:345–358.

Leutgeb S, Leutgeb JK (2007) Pattern separation, pattern completion, and new neuronal codes within a continuous CA3 map. Learning & Memory 14:745–757.

Li S-C, Lindenberger U, Sikström S (2001) Aging cognition: from neuromodulation to representation. Trends Cogn Sci 5:479–486.

Logan J (2000) Graphical analysis of PET data applied to reversible and irreversible tracers. Nucl Med Biol 27:661–670.

Marks SM, Lockhart SN, Baker SL, Jagust WJ (2017) Tau and β-amyloid are associated with medial temporal lobe structure, function, and memory encoding in normal aging. J Neurosci 37:3192–3201.

Marr D (1971) Simple memory: a theory for archicortex. Phil Trans R Soc B 262:23–81.

Mathalon DH, Sullivan EV, Rawles JM, Pfefferbaum A (1993) Correction for head size in brain-imaging measurements. Psychiatry Res Neuroimaging 50:121–139.

Mattson MP, Cheng B, Davis D, Bryant K, Lieberburg I, Rydel RE (1992) β-Amyloid peptides destabilize calcium homeostasis and render human cortical neurons vulnerable to excitotoxicity. J Neurosci 12:376–389.

Miller SL, Celone K, DePeau K, Diamond E, Dickerson BC, Rentz D, Pihlajamaki M, Sperling RA (2008) Age-related memory impairment associated with loss of parietal deactivation but preserved hippocampal activation. Proc Natl Acad Sci USA 105:2181–2186.

Mormino EC, Brandel MG, Madison CM, Marks SM, Baker SL, Jagust WJ (2012) Aβ deposition in aging is associated with increases in brain activation during successful memory encoding. Cereb Cortex 22:1813–1823.

Mormino EC, Smiljic A, Hayenga AO, Onami SH, Greicius MD, Rabinovici GD, Janabi M, Baker SL, Yen IV, Madison CM, Miller BL, Jagust WJ (2011) Relationships between β-amyloid and functional connectivity in different components of the default mode network in aging. Cereb Cortex 21:2399–2407.

Moscovitch M, Cabeza R, Winocur G, Nadel L (2016) Episodic memory and beyond: The hippocampus and neocortex in transformation. Annu Rev Psychol 67:105–134.

Nicolle MM, Colombo PJ, Gallagher M, McKinney M (1999) Metabotropic glutamate receptor-mediated hippocampal phosphoinositide turnover is blunted in spatial learning-impaired aged rats. J Neurosci 19:9604–9610.

Norman KA, O'Reilly RC (2002) Modeling hippocampal and neocortical contributions to recognition memory: a complementary-learning-systems approach. Psychol Rev 110:611–646.

O'Reilly RC, McClelland JL (1994) Hippocampal conjunctive encoding, storage, and recall: avoiding a trade-off. Hippocampus 4:661–682.

O'Reilly RC, Norman KA (2002) Hippocampal and neocortical contributions to memory: advances in the complementary learning systems framework. Trends Cogn Sci 6:505–510.

Oddo S, Caccamo A, Shepherd JD, Murphy MP, Golde TE, Kayed R, Metherate R, Mattson MP, Akbari Y, LaFerla FM (2003) Triple-transgenic model of Alzheimer's disease with plaques and tangles: intracellular Abeta and synaptic dysfunction. Neuron 39:409–421.

Oh H, Jagust WJ (2013) Frontotemporal network connectivity during memory encoding is increased with aging and disrupted by beta-amyloid. J Neurosci 33:18425–18437.

Ong W-Y, Tanaka K, Dawe GS, Ittner LM, Farooqui AA (2013) Slow excitotoxicity in Alzheimer's disease. J Alzheimers Dis 35:643–668.

Ossenkoppele R et al. (2016) Tau PET patterns mirror clinical and neuroanatomical

variability in Alzheimer’s disease. Brain 139:1551–1567.

Palop JJ, Chin J, Roberson ED, Wang J, Thwin MT, Bien-Ly N, Yoo J, Ho KO, Yu G-Q, Kreitzer A, Finkbeiner S, Noebels JL, Mucke L (2007) Aberrant excitatory neuronal activity and compensatory remodeling of inhibitory hippocampal circuits in mouse models of Alzheimer's disease. Neuron 55:697–711.

Persson J, Kalpouzos G, Nilsson L-G, Ryberg M, Nyberg L (2010) Preserved hippocampus activation in normal aging as revealed by fMRI. Hippocampus 21:753–766.

Price JC, Klunk WE, Lopresti BJ, Lu X, Hoge JA, Ziolko SK, Holt DP, Meltzer CC, DeKosky ST, Mathis CA (2005) Kinetic modeling of amyloid binding in humans using PET imaging and Pittsburgh Compound-B. J Cereb Blood Flow Metab 25:1528–1547.

Price JL, Morris JC (1999) Tangles and plaques in nondemented aging and “preclinical” Alzheimer's disease. Ann Neurol 45:358–368.

Pruessner JC, Collins DL, Pruessner M, Evans AC (2001) Age and gender predict volume decline in the anterior and posterior hippocampus in early adulthood. J Neurosci 21:194–200.

Pruessner JC, Köhler S, Crane J, Pruessner M, Lord C, Byrne A, Kabani N, Collins DL, Evans AC (2002) Volumetry of temporopolar, perirhinal, entorhinal and parahippocampal cortex from high-resolution MR images: considering the variability of the collateral sulcus. Cereb Cortex 12:1342–1353.

Putcha D, Brickhouse M, O'Keefe K, Sullivan C, Rentz D, Marshall G, Dickerson B, Sperling RA (2011) Hippocampal hyperactivation associated with cortical thinning in Alzheimer's disease signature regions in non-demented elderly adults. J Neurosci 31:17680–17688.

Ranganath C, Ritchey M (2012) Two cortical systems for memory-guided behaviour. Nat Rev Neurosci 13:713–726.

Rapoport M, Dawson HN, Binder LI, Vitek MP, Ferreira A (2002) Tau is essential to beta-amyloid-induced neurotoxicity. Proc Natl Acad Sci USA 99:6364–6369.

Raz N, Rodrigue KM, Head D, Kennedy KM, Acker JD (2004) Differential aging of the medial temporal lobe. Neurology 62:433–438.

Roberson ED, Halabisky B, Yoo JW, Yao J, Chin J, Yan F, Wu T, Hamto P, Devidze N, Yu G-Q, Palop JJ, Noebels JL, Mucke L (2011) Amyloid-β/Fyn-induced synaptic, network, and cognitive impairments depend on tau levels in multiple mouse models of Alzheimer's disease. J Neurosci 31:700–711.

Roberson ED, Scearce-Levie K, Palop JJ, Yan F, Cheng IH, Wu T, Gerstein H, Yu G-Q,

Mucke L (2007) Reducing endogenous tau ameliorates amyloid β-induced deficits in an Alzheimer's disease mouse model. Science 316:750–754.

Rolls ET (1996) A theory of hippocampal function in memory. Hippocampus 6:601–620.

Rousset OG, Ma Y, Evans AC (1998) Correction for partial volume effects in PET: principle and validation. J Nucl Med 39:904–911.

Saint-Aubert L, Almkvist O, Chiotis K, Almeida R, Wall A, Nordberg A (2016) Regional tau deposition measured by [(18)F]THK5317 positron emission tomography is associated to cognition via glucose metabolism in Alzheimer's disease. Alzheimers Res Ther 8:1–9.

Schacter DL, Tulving E (1994) What are the memory systems of 1994? In: Memory systems (Tulving E, Schacter DL, eds), pp 1–39. Cambridge.

Scheltens P (2001) Structural neuroimaging of Alzheimer’s disease and other dementias. Aging Clin Exp Res 13:203–209.

Schöll M, Lockhart SN, Schonhaut DR, O'Neil JP, Janabi M, Ossenkoppele R, Baker SL, Vogel JW, Faria J, Schwimmer HD, Rabinovici GD, Jagust WJ (2016) PET imaging of tau deposition in the aging human brain. Neuron 89:971–982.

Schwarz AJ, Yu P, Miller BB, Shcherbinin S, Dickson J, Navitsky M, Joshi AD, Devous MD Sr, Mintun MS (2016) Regional profiles of the candidate tau PET ligand 18F-AV-1451 recapitulate key features of Braak histopathological stages. Brain 139:1539–1550.

Ségonne F, Dale AM, Busa E, Glessner M, Salat D, Hahn HK, Fischl B (2004) A hybrid approach to the skull stripping problem in MRI. NeuroImage 22:1060–1075.

Shankar GM, Bloodgood BL, Townsend M, Walsh DM, Selkoe DJ, Sabatini BL (2007) Natural oligomers of the Alzheimer amyloid-beta protein induce reversible synapse loss by modulating an NMDA-type glutamate receptor-dependent signaling pathway. J Neurosci 27:2866–2875.

Small SA, Stern Y, Tang M, Mayeux R (1999) Selective decline in memory function among healthy elderly. Neurology 52:1392–1396.

Smith TD, Adams MM, Gallagher M, Morrison JH, Rapp PR (2000) Circuit-specific alterations in hippocampal synaptophysin immunoreactivity predict spatial learning impairment in aged rats. 20:6587–6593.

Sperling RA (2007) Functional MRI studies of associative encoding in normal aging, mild cognitive impairment, and Alzheimer's disease. Annals of the New York Academy of Sciences 1097:146–155.

Sperling RA, Bates JF, Chua EF, Cocchiarella AJ, Rentz DM, Rosen BR, Schacter DL,

Albert MS (2003) fMRI studies of associative encoding in young and elderly controls and mild Alzheimer's disease. J Neurol Neurosurg Psychiatry 74:44–50.

Sperling RA, LaViolette PS, O'Keefe K, O'Brien J, Rentz DM, Pihlajamaki M, Marshall G, Hyman BT, Selkoe DJ, Hedden T, Buckner RL, Becker JA, Johnson KA (2009) Amyloid deposition is associated with impaired default network function in older persons without dementia. Neuron 63:178–188.

Spires-Jones TL, Hyman BT (2014) The intersection of amyloid beta and tau at synapses in Alzheimer's disease. Neuron 82:756–771.

Squire LR (1992) Memory and the hippocampus: a synthesis from findings with rats, monkeys, and humans. Psychol Rev 99:195–231.

Squire LR, Zola SM (1996) Structure and function of declarative and nondeclarative memory systems. Proc Natl Acad Sci USA 93:13515–13522.

Stanley DP, Shetty AK (2004) Aging in the rat hippocampus is associated with widespread reductions in the number of glutamate decarboxylase-67 positive interneurons but not interneuron degeneration. J Neurochem 89:204–216.

Thal DR, Rub U, Orantes M, Braak H (2002) Phases of Aβ-deposition in the human brain and its relevance for the development of AD. Neurology 58:1791–1800.

Tomlinson BE, Blessed G, Roth M (1968) Observations on the brains of non-demented old people. J Neurol Sci 7:331–356.

Tompary A, Duncan K, Davachi L (2016) High-resolution investigation of memory-specific reinstatement in the hippocampus and perirhinal cortex. Hippocampus 26:995–1007.

Treves A, Rolls ET (1994) Computational analysis of the role of the hippocampus in memory. Hippocampus 4:374–391.

Tulving E (1972) Episodic and semantic memory. In: Organization of memory (Tulving E, Donaldson W, eds), pp 381–403. Academic Press.

Tulving E (2002) Episodic memory: from mind to brain. Annu Rev Psychol 53:1–25.

Tulving E, Hayman CA, Macdonald CA (1991) Long-lasting perceptual priming and semantic learning in amnesia: A case experiment. J Exp Psychol Learn Mem Cogn 17:595–617.

Tulving E, Markowitsch HJ (1998) Episodic and declarative memory: role of the hippocampus. Hippocampus 8:198–204.

van den Honert RN, McCarthy G, Johnson MK (2016) Reactivation during encoding supports the later discrimination of similar episodic memories. Hippocampus

26:1168–1178.

van Rossum IA, Visser PJ, Knol DL, van der Flier WM, Teunissen CE, Barkhof F, Blankenstein MA, Scheltens P (2012) Injury markers but not amyloid markers are associated with rapid progression from mild cognitive impairment to dementia in Alzheimer's disease. J Alzheimers Dis 29:319–327.

Vannini P, Hedden T, Becker JA, Sullivan C, Putcha D, Rentz D, Johnson KA, Sperling RA (2012a) Age and amyloid-related alterations in default network habituation to stimulus repetition. Neurobiol Aging 33:1237–1252.

Vannini P, Hedden T, Sullivan C, Sperling RA (2012b) Differential functional response in the posteromedial cortices and hippocampus to stimulus repetition during successful memory encoding. Hum Brain Mapp 34:1568–1578.

Vela J, Gutierrez A, Vitorica J, Ruano D (2003) Rat hippocampal GABAergic molecular markers are differentially affected by ageing. J Neurochem 85:368–377.

Villeneuve S et al. (2015) Existing Pittsburgh Compound-B positron emission tomography thresholds are too high: statistical and pathological evaluation. Brain 138:2020–2033.

Walsh DM, Klyubin I, Fadeeva JV, Cullen WK, Anwyl R, Wolfe MS, Rowan MJ, Selkoe DJ (2002) Naturally secreted oligomers of amyloid beta protein potently inhibit hippocampal long-term potentiation in vivo. Nature 416:535–539.

Wilson IA, Ikonen S, Gallagher M, Eichenbaum H, Tanila H (2005) Age-associated alterations of hippocampal place cells are subregion specific. J Neurosci 25:6877–6886.

Wilson IA, Ikonen S, McMahan RW, Gallagher M, Eichenbaum H, Tanila H (2003) Place cell rigidity correlates with impaired spatial learning in aged rats. 24:297–305.

Xia C-F et al. (2013) [18F]T807, a novel tau positron emission tomography imaging agent for Alzheimer's disease. Alzheimers Dement 9:666–676.

Yassa MA, Lacy JW, Stark SM, Albert MS, Gallagher M, Stark CEL (2011a) Pattern separation deficits associated with increased hippocampal CA3 and dentate gyrus activity in nondemented older adults. Hippocampus 21:968–979.

Yassa MA, Mattfeld AT, Stark SM (2011b) Age-related memory deficits linked to circuit-specific disruptions in the hippocampus. In, pp 8873–8878.

Yassa MA, Muftuler LT, Stark CEL, Squire LR (2010a) Ultrahigh-resolution microstructural diffusion tensor imaging reveals perforant path degradation in aged humans in vivo. Proc Natl Acad Sci USA 107:12687–12691.

Yassa MA, Stark SM, Bakker A, Albert MS, Gallagher M, Stark CEL (2010b) High-

resolution structural and functional MRI of hippocampal CA3 and dentate gyrus in patients with amnestic mild cognitive impairment. NeuroImage 51:1242–1252.

Yonelinas AP (2002) The nature of recollection and familiarity: a review of 30 years of research. Journal of Memory and Language 46:441–517.

Yonelinas AP, Aly M, Wang W-C, Koen JD (2010) Recollection and familiarity: Examining controversial assumptions and new directions Voss JL, Paller KA, eds. Hippocampus 20:1178–1194.